**β–substituted $Zn^{II}$ porphyrins as dyes for DSSC: a possible approach to photovoltaic windows.**

Gabriele Di Carlo,[a] Alessio Orbelli Biroli,[b] Francesca Tessore,[a] Stefano Caramori,[c] Maddalena Pizzotti,[a]*

[a] *Department of Chemistry, University of Milan, INSTM Research Unit, Via C. Golgi 19, 20133 Milano (Italy)*
[b] *Istituto di Scienze e Tecnologie Molecolari del CNR (CNR-ISTM), SmartMatLab Centre, Via C. Golgi 19, 20133 Milano (Italy)*
[c] *Department of Chemistry and Pharmaceutical Sciences and #ISOF/CNR c/o Department of Chemistry and Pharmaceutical Sciences, University of Ferrara, Via Fossato di Mortara 17, 44121 Ferrara, Italy*

***Corresponding Author**: Maddalena Pizzotti, Department of Chemistry, University of Milan, INSTM Research Unit, Via C. Golgi 19, 20133 Milano (Italy). e-mail: maddalena.pizzotti@unimi.it

**Abstract**

The development of building integrated photovoltaic (BIPV) technology and its implementation in construction of the building envelop provide aesthetical, economical and technical solutions toward the zero-energy building. In this perspective Dye-Sensitized Solar Cells (DSSCs), which can be obtained in transparent form and with tunable different colors, offer not only an alternative to the traditional silicon solar cells to be applied in particular to decorative effects on windows and glass integrated façades, but also to indoor structures (and furnishings) in order to recapture the energy spent for the inner lighting, thanks to their peculiar ability of operating in diffuse light condition.

In this context, porphyrin-based molecules have an immense potential as light harvesting component of dye-sensitized nanocrystalline $TiO_2$ solar cells, reaching now efficiencies up to about 13 %. However the multistep synthesis of the best performing porphyrin dyes, showing a *meso*

substitution pattern, is characterized by very low overall yields compromising their possible applicative development for instance in large photovoltaic (PV) glass modules in competition with the actual commercial PV glass modules based on $CuInGaSe_2$ or CdTe thin voltaic films.

In this review the renewed interest in the role of the β-substituted $Zn^{II}$ porphyrins for PV application, less studied than the *meso* substituted ones, is highlighted. Indeed they can rely on a more accessible synthetic procedure since their tetraaryl porphyrinic core can be easily obtained by a one pot reaction between pyrrole and the appropriate aryl aldehyde. Moreover, their remarkable light harvesting properties in the visible range as well as their peculiar steric hindrance, which strongly opposes to the charge recombination process at the photoanode/dye/electrolyte interface, make this kind of cost-effective porphyrinic dyes more promising for application in new PV glass modules based on DSSC technology, to be applied BIPV.

**Keywords:** DSSC, building-integrated photovoltaics, Zn porphyrins, β substituted porphyrins

## 1. Introduction

The first installation of photovoltaic (PV) modules as glass elements integrated into a wall façade with isolating glass was realized in 1991. Since then the building-integrated photovoltaics (BIPV) developed quite rapidly. Today a standard-size module for PV façades or roof installations reaches 1 MW output [1].

Commercial BIPV glass modules are constituted by a thin layer of mono or multi solar cells, based on the traditional crystalline or amorphous silicon semiconductor embedded into resin foils between two glass planes. Although the actual commercial solutions already give some interesting advantages such as day-lighting, shading, noise reduction and, most relevant, electricity production, there is in the modern architecture an increasing demand for alternative PV glass modules, which can introduce new decorative and specific lighting solutions [2].

These solutions could offer a high degree of freedom for the design (not only geometric) and aesthetics of a building integrated module. With this objective, since the last 10-15 years dye-sensitized solar cell (DSSC) technology has been considered as a potential basis of new building integrated PV modules. In fact, starting from the pioneering work by Grätzel et al. in 1991 [3], DSSCs have emerged as an alternative to conventional silicon-based solar cells, being low cost photovoltaic devices with interesting power conversion efficiency. Since DSSCs can be obtained in transparent form and with tunable different colors, they can be potentially interesting for their application in PV glass integrated façades or "smart" windows [4-10].

Moreover DSSCs are characterized by the peculiar ability of operating also in diffuse light condition [11]. This feature can be exploited for the internal structures (e.g. transparent walls [12]), doors or furnishings in order to obtain a recovery of the energy spent for the internal lighting.

Such a versatile applicability to outdoor/indoor environmental makes DSSC a potential solution to satisfy the technological requirement for the integration of renewable energy resources in construction of the building envelop and toward the definition of the zero-energy-building standards [13, 14], as required by several countries by 2020, in order to contribute in the limiting of the greenhouse gas emission [15].

The standard design of a DSSC comprises a dye sensitized photoanode ($TiO_2$) and a platinum counter electrode with a liquid electrolyte redox mediator (for example based on $I_3^-/I^-$, $Co^{II}/Co^{III}$ or more recently on $Cu^{+/2+}$ [16]) filling the space between anode and cathode (Figure 1).

By photoexcitation an electron is transferred to the excited state orbitals of the dye, followed by injection of the excited electron into the conduction band of the $TiO_2$ semiconductor, resulting in the oxidation of the dye. The injected electron diffuses through the $TiO_2$ photoanode toward the transparent conducting glass and reaches a platinum counter electrode through the external wiring. The oxidized dye is then reduced by means of a process involving for instance the $I^-$ ions of the

electrolytic mediator, regenerating its ground state, while the resulting $I_3^-$ ions are reduced to $I^-$ ions by the counter electrode, in this way completing the electrical circuit (Figure 1).

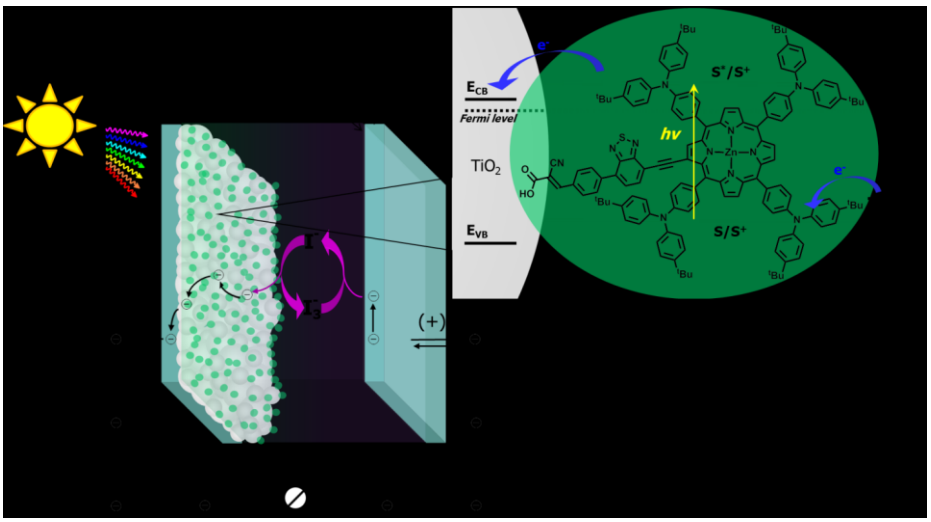


**Figure 1.** Schematic diagram illustrating the working principle of a DSSC

Initially, ruthenium complexes have been the most efficient dyes (**N3** [17] and **N719** [18]) showing a power conversion efficiency up to 11% [17-19], however the high cost and the limited supply of ruthenium, together with the poor absorption of these dyes in the near infrared region limited their widespread application. On the other hand organic metal-free dyes have reached power efficiency of 14% in DSSCs co-sensitized with the organic dyes **ADEKA-1** and **LEG-4** [20].

Photosynthesis, the natural process through which plants convert sunlight into chemical energy, represents one of the more relevant photophysical natural processes, where chlorophylls, containing several porphyrin molecules, play the role of light harvesting antennae. As a consequence a large interest in metal porphyrins as dyes or in general as antennae was raised, by virtue of their strong electronic absorption bands at around 500 and beyond 600 nm and their long lived $\pi^*$ singlet excited states of appropriate LUMO energy, to allow injection of the excited electron into the $TiO_2$

semiconductor. They have also the advantage of a molecular structure with many reaction sites, four *meso* and eight β pyrrolic positions, which can be functionalized, allowing fine tuning of their electronic and photophysical properties. Until 2010, the energy conversion efficiency for DSSC based on porphyrinic dyes was much lower than those based on ruthenium complexes, but the development of porphyrinic push-pull systems with a strong directional HOMO-LUMO transition around 600 nm and the introduction of bulky substituents into the porphyrinic structure in order to avoid π–π aggregation on the photoanode, have significantly improved the efficiencies of the DSSCs based on $Zn^{II}$ porphyrin dyes up to 12.3% [21] with the porphyrinic dye **YD2-oC8** co-sensitized with an organic dye (**Y123**) and of about 13% with the push-pull porphyrinic dyes **SM315** [22] and **GY50** [23], using in all cases, as redox mediator, a cobalt based redox couple (Figure 2).

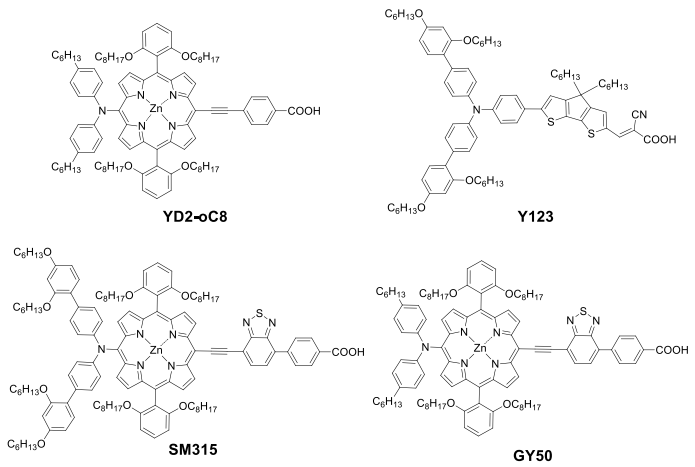


**Figure 2.** Molecular structures of **YD2-oC8** and **Y123** [21] (η=12.3%) green, **SM315** [22] (η = 13.0%) brown and **GY50** [23] (η=13.15 %)

On the basis of these latter results, 5,15 *meso* disubstituted push-pull $Zn^{II}$ porphyrins, characterized by a strong and directional charge transfer process along the push-pull system, were considered as

the best porphyrinic structures allowing high DSSC efficiencies [24]. However their syntheses, which require multiple steps, are characterized by very low overall yields [25-29], (9-32% starting from porphyrin core and depending on complexity of the structure) making difficult to imagine a possible applicative development for instance in PV glass modules to be integrated in building façades or in "smart" windows [1].

On the other hand, β substituted tetraaryl $Zn^{II}$ porphyrins can rely on a symmetric core, easily obtained by a one pot reaction between pyrrole and the appropriate aryl aldehyde, making them synthetically less demanding. Moreover, the attachment of an appropriate functional substituent to the β pyrrolic position, such as a π-ethynyl phenyl system carrying a carboxylic ending group, can be now obtained by a rather simple synthetic approach [24], so that a new class of β substituted porphyrinic dyes could be probably quite suitable for large scale production necessary for the development of colored PV glass modules based on DSSC technology. Despite an encouraging efficiency (η) of 7.1 % has been attained already in 2007 by the pale green β-substituted tetraaryl $Zn^{II}$ porphyrin **1** (Figure 3) [30], this series of porphyrins has been less investigated as dyes for DSSC. Most likely this was due to the difficulty in getting an efficient donor-acceptor system through the β-architecture. However, in the last decade, many efforts have been devoted to address such a problem and novel porphyrin dyes have been rationally designed to improve the push-pull character of β-substituted tetraaryl $Zn^{II}$ porphyrins [24, 31-33].

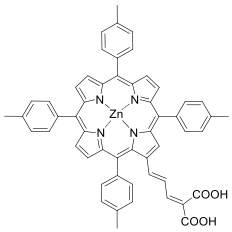


**1**

**Figure 3.** Chemical structure of **1** [30] (η=7.1 %) green

In addition a large part of the β-substituted porphyrinic dyes is characterized by a pale green color (see later) excellent for new colored PV glass modules to be integrated into smart windows, both for aesthetic reasons and a pleasant internal lighting. Recent advances in the porphyrin-based DSSCs have been reported up to now in several Reviews [4, 5, 7, 9, 10, 34, 35] together with detailed studies on their photophysical properties including for example a series of mechanicistic studies on the electron transfer processes [36] and on the relevance of different anchoring groups to the photoanode [37]. However very little attention has been devoted to an evaluation of their practical potential applications, such as in colored photovoltaic "smart windows" where 7-8% power efficiency appears satisfying enough if the cost of the dye is relatively low.

Therefore this short review is not only focused on a survey of DSSCs based on β-pyrrolic substituted $Zn^{II}$ porphyrins, but also on a preliminary evaluation of their potential applications in PV glass modules for "smart windows" to be applied, for both aesthetic and specific lighting requirements, in BIPV.

## 2. Synthesis

The high versatility of $Zn^{II}$ porphyrins as dyes in DSSCs is ascribed to their tunable molecular structure. In fact, the four *meso* and the eight β-pyrrolic positions, available in the porphyrinic ring, open several opportunities of chemical modification of their electronic structure for a fine modulation of the absorption, electrochemical, emission and photophysical properties. The tuning of such properties can be achieved by well-controlled modification of the position and nature of the substituents thus obtaining rather complex and often highly asymmetric porphyrinic structures. Hitherto several highly asymmetrical $Zn^{II}$ porphyrins have been synthesized, as dyes for DSSC, with the aim to enhance their charge transfer character, mainly by a push-pull 5,15 disubstituted system [38], in order to improve both the charge transfer processes and the light harvesting efficiency [37, 39-41], reaching, in some cases, remarkable DSSC performances. However their

arduous synthetic pathways limit the scale-up of their synthesis. Therefore many efforts have been made so far, in order to get by easier synthetic approaches, porphyrinic structures still maintaining an appropriate charge transfer character and a significant light harvesting efficiency.

In 2011, within a comprehensive review, Senge [42] reported a range of synthetic approaches for highly asymmetric ABCD-type porphyrins bearing mixed substituents (A, B, C, D) in *meso* positions. He mainly focused the attention on three different procedures consisting of *i) mixed condensation, ii) total synthesis,* and *iii) functionalization of preformed systems*. The mixed condensation involves a one-pot condensation of pyrrole with four different aldehydes providing a statistical mixture of various isomers from which the highly asymmetric A,B,C,D target is obtained in very low yields by chromatography separation.

The total synthesis, on the other hand, requires a large number of synthetic steps, making this approach far from trivial.

The last method requires a tedious step-by-step introduction of the desired substituents into an unsubstituted porphyrinic core.

Lindsey has surveyed several synthetic routes to produce asymmetrical 5,15 -AB-type *meso*-patterned porphyrins [43]. However, the classical mixed condensation method, when used to introduce two different types of substituents in *meso*-positions is characterized by "*high temperature reactions, limited scope of substituents and statistical mixtures accompanied by laborious chromatography. Such methods left unrealized the tremendous utility of meso-substituted porphyrins across the enormously broad field of porphyrin science,…"* [43]. As opposed the typical pathway for the synthesis of 5,15 -AB-type *meso* $Zn^{II}$ porphyrins, which have reached, so far, the best performances as dyes in DSSC [21, 22], consists of a first condensation step between formaldehyde and pyrrole to give the unsubstituted dipyrromethane with acceptable yields (up to 50%), followed by a second condensation step with an appropriate arylaldehyde to produce the basic starting 10,20 bisaryl $A_2$-type porphyrinic core (yield up to 50% depending on arylaldehyde). A bromination step on the two 5,15-*meso* positions yields a valuable building block for their

asymmetric subsequent functionalization, to produce a push-pull donor-acceptor system. The donor (D) and acceptor (A) substituents, due to their different reactivity, must be introduced sequentially, thus making the synthetic procedure rather ineffective [21, 22].

Indeed, when the bromine atoms in 5,15-*meso* positions are replaced with donor and acceptor acetylenic derivatives *via* two subsequent Sonogashira coupling reactions, statistical mixtures of *meso* disubstituted symmetrical and asymmetrical porphyrins are obtained (Scheme 1, A). The pathway to introduce step by step an amine donor group at one end and an ethynyl-based acceptor at the other end of the push-pull system (Scheme 1, B) is even more complex. One of the bromine atoms in *meso*-position is first replaced with an alkyl silyl ethynyl substituent *via* a Sonogashira coupling reaction and the other one is reacted with a diaryl amine by a Buchwald-Hartwig cross coupling reaction. The subsequent cleavage of the protecting alkyl silyl group, providing the terminal ethynyl residue, enables to react with the aromatic acceptor unit by a final Sonogashira coupling [21, 22].

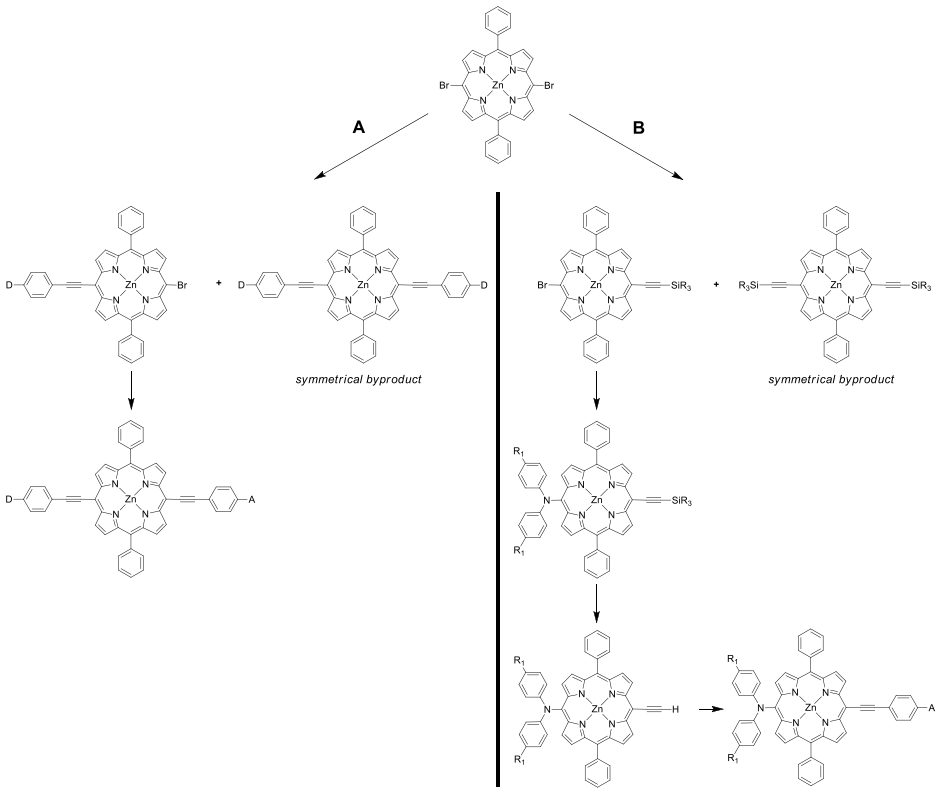


**Scheme 1.** Synthesis of 5,15 AB-type porphyrins

Despite such long and rather ineffective synthetic pathways, push-pull 5,15-disubstituted $Zn^{II}$ porphyrins have been extensively investigated as dyes for DSSC, reaching conversion efficiencies exceeding 13% by using $Co^{2+/3+}$ trisbipyridine complexes as redox shuttles.[21-23] The use of cobalt-based electrolytic mediators makes mandatory the enveloping of the porphyrinic core by hydrophobic alkoxy chains in order to suppress the charge recombination rate on the photoanode thus improving the electron transfer process. Moreover also dye aggregation on the $TiO_2$ surface is prevented, favouring the power conversion efficiency [44]. As a result, despite they have shown remarkable conversion efficiencies, their synthetic procedure became even more laborious reducing again the overall yields. For this reason, a growing interest has been recently devoted in achieving less structurally complex porphyrinic dyes [45].

However all the synthetic procedures reported in Scheme 1 do not allow a scale-up of the production of this kind of $Zn^{II}$ porphyrinic dyes to a multi-gram scale which is mandatory for the development of DSSCs in BIPV applications. Thanks to their straightforward and effective synthetic procedures along with the tunability of their electronic properties by rather simple structural modification, an increasing interest has been recently devoted to the development of $Zn^{II}$ porphyrins with a β-substitution pattern with the most relevant series based on the symmetrical 5,10,15,20-tetraarylporphyrinic core [24, 30, 32, 34, 35, 37, 46]. The latter can be easily obtained in excellent yields (from 10% to over 50% depending on steric hindrance of the arylaldehyde) by an easy one-pot condensation between pyrrole and suitable aldehydes. Functionalization of one β pyrrolic position by a bromine atom [47] or an aldehyde group [30], followed by a rather simple insertion of a π acceptor substituent carrying an anchoring -COOH group yields β substituted porphyrinic dyes by a synthetic route much less demanding and thus more viable for a multi-gram scale production.

Unexpectedly, up to recently few examples of such type of $Zn^{II}$ porphyrinic dyes have been investigated, although, since 2004, Officer and co-workers [5, 30, 48] reported a number of tetrarylporphyrins carrying olefin-linked electron acceptor substituents in β-pyrrolic position, reaching 7.1% conversion efficiency with the dye **1** (Figure 3). For this specific dye the porphyrin ring is easily obtained by the typical Lindsey conditions [49], the subsequent selective formylation of one β pyrrolic position, which first requires the introduction of a $Cu^{II}$ ion into the porphyrinic ring, is achieved by Vilsmeier reaction. After decomplexation, a Wittig reaction between the aldehyde and acetic esters of phosphanylidene derivatives introduces the first ethenyl bond. The extension of the π-system involves sequential reduction of the ester, its oxidation into aldehyde and a further Wittig reaction. Introduction of the $Zn^{II}$ ion into the porphyrinic core followed by the Knovenagel condensation of terminal aldehyde with malonic or cyanoacetic acids gives the $Zn^{II}$ porphyrin dye in good yields (32-50% depending on the pendant extension) (Scheme 2).

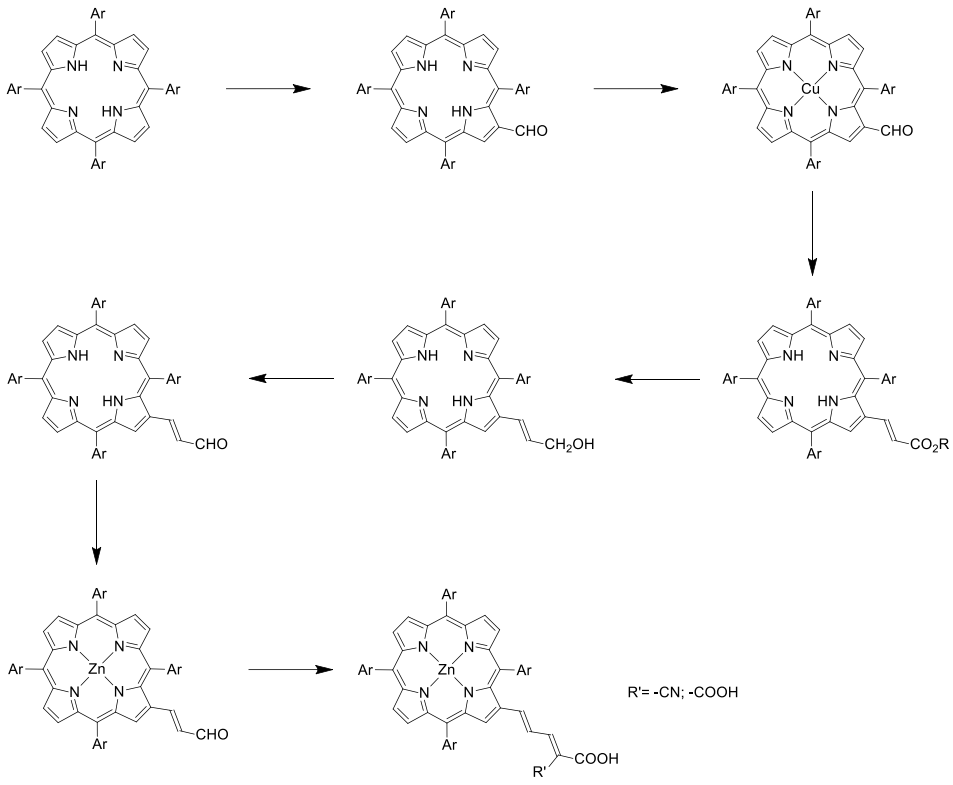


**Scheme 2.** Synthetic pathway to β-ethenyl and butadienyl substituted tetraaryl $Zn^{II}$ porphyrins

Other β-ethenyl substituted $Zn^{II}$ porphyrins have been recently reported by Ishida et al [50, 51], providing novel dyes based on a donor-*meso*-substituted β-functionalized structure. This rather atypical geometry needs a complex synthetic pathway starting from the synthesis of the 10,20-diarylsubstituted porphyrinic core (Scheme 3). Bromination at one *meso* position and insertion of $Zn^{II}$ ion, followed by functionalization with a diarylamine unit by a Buchwald-Hartwig reaction, gives an asymmetric trisubstituted intermediate. The β substitution is obtained by a selective iridium-catalyzed borylation of the pyrrolic position followed by a rhodium or palladium-catalyzed

Heck-reaction with a number of vinyl esters, providing, after hydrolysis, the desired push-pull porphyrinic dyes. When sensitized with these dyes, both iodine and cobalt-based mediators DSSCs have shown good conversion efficiencies [50, 51].

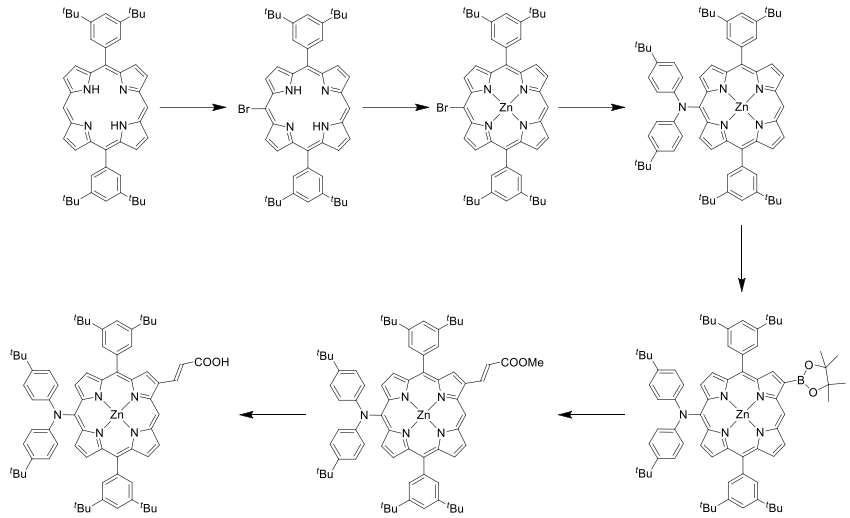


**Scheme 3.** Synthetic pathway to donor-*meso*-substituted β-functionalized $Zn^{II}$ porphyrins

An intriguing procedure for the synthesis of $Zn^{II}$ porphyrins β substituted by an acetylenic acceptor unit with overall yields ranging from moderate to high has been reported by Partridge *et al*. [52] (Scheme 4A).

This synthetic procedure can be applied to a range of symmetrical and non-symmetrical β substituted $Zn^{II}$ porphyrins *via* a first formylation step at the β pyrrolic position followed by a modified Horner–Emmons condensation. However this last step cannot be applied when functional groups such as carboxylic or cyanoacrylic acids are involved. More recently some of us have optimized synthetic procedures to directly introduce in β position acetylenic derivatives bearing carboxylic or cyanoacrylic groups [24]. The one-pot cyclization step to produce the 5,10,15,20-tetrakis(3,5-di-*tert*-butyl-phenyl) porphyrinic core is followed by the bromination at the β pyrrolic

position and introduction of the $Zn^{II}$ ion [46]. The direct introduction of the carboxylic-based ethynyl moiety is successfully achieved by an assisted microwave Sonogashira coupling reaction reaching a two-fold yield in comparison to the reported procedure involving the thermal approach [24] (Scheme 4B).

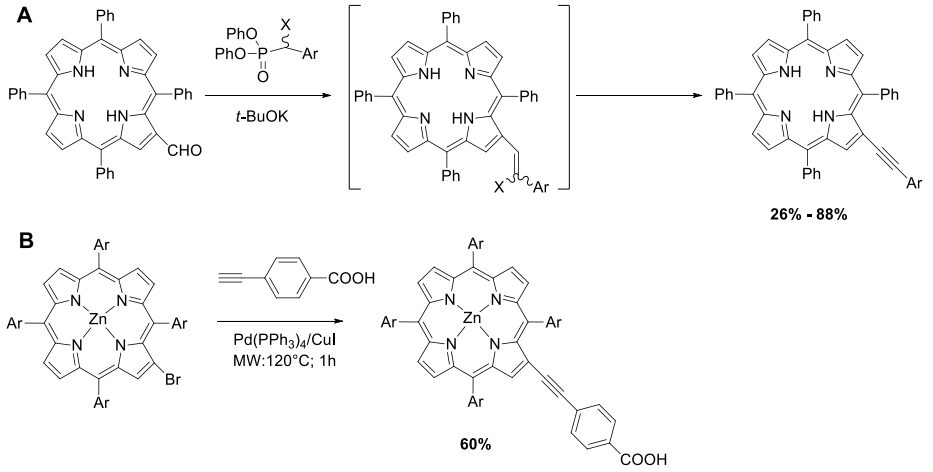


**Scheme 4.** A) modified Horner–Emmons condensation; B) assisted microwave Sonogashira coupling reaction

By applying the same strategy at the 2,12 dibromo $Zn^{II}$ porphyrinic structure, acetylenic substituents with an electron donating group at one end and an electron withdrawing group at the other end have been introduced in a single step reaction producing the first example of a push–pull system on β-positions (see later Figure 16) [24]. Despite the statistical distribution of the reaction products, the push-pull asymmetric 2,12 $Zn^{II}$ porphyrin is obtained in acceptable yields, (23%) after a quite easy chromatographic separation and purification. The selective bromination of the starting porphyrin core at 2,12 positions has been optimized very recently [46].

More complex structures based on β-multi-substituted $Zn^{II}$ porphyrins with a rather unusual push-pull fused system on the four opposed pyrrolic positions have been synthesised both by Imahori [53] and Wang [54, 55], showing, in some cases, a satisfactory DSSC efficiency [53]. Their

synthetic route is complex and involves a series of Heck reactions, followed by cyclisation of the alkene substituents and final aromatization by oxidation to obtain fused systems. As we will see later, this type of condensed structures, which require a complex synthetic pathway, do not really fit in with the aims of this review.

The introduction of alkoxy chains in different positions of the four aryl rings of $Zn^{II}$ tetrarylporphyrins has been recently investigated with the aim of a rational design of β substituted $Zn^{II}$ porphyrinic dyes showing improved photoelectrochemical properties [32, 56]. Sterically hindered bulky porphyrinic cores have been synthesized by cyclization of pyrrole with various alkoxy wrapped benzaldehydes. In the peculiar case of the *ortho*,*ortho* dialkoxy benzaldehyde, much more reactive than *ortho*, *para* and *ortho* substituted benzaldehydes, the addition of a heterogeneous $In^{III}$-salt acting as catalyst to promote the cyclization, was necessary, since a fast polymerization has been observed when usual Lindsey's acidic catalysts [49], like $CF_3COOH$ or $BF_3{\cdot}OEt_2$, were employed. The bromination at one pyrrolic position followed by insertion of the $Zn^{II}$ ion and by the introduction of the acetylenic acceptor moiety via microwave assisted Sonogashira coupling reaction, yielded the β substituted dyes (from 11% to 55% depending on the steric hindrance of the porphyrin core) [32, 56].

With the specific purpose to achieve a more significant charge-separation character a novel 4D-π-1A type porphyrinic structure has been synthesised very recently [33]. Arylamino donating groups have been inserted in *meso* position to increase the electron density on the $Zn^{II}$ porphyrinic core [40, 57] and two acceptor substituents have been surveyed in β position. The synthetic approach involved the one-pot cyclization between 4-bromobenzaldehyde and pyrrole followed by multiple Buchwald-Hartwig aminations of the tetra(4-bromophenyl)porphyrin. After introduction of the $Zn^{II}$ ion, the resulting $Zn^{II}$ tetra(arylamino)porphyrinic core has been functionalized at the β-position by NBS bromination step. The microwave assisted Sonogashira coupling of the brominated core with an ethynyl moiety carrying an aldehyde group and the following Knoevenagel condensation of this

latter with cyanoacetic acid afforded dye **2** (Scheme 5). When an auxiliary electron withdrawing group such as a benzotiadiazole moiety (BTD) has been introduced in the β pendant as in **3**, the increased push-pull character of the 4D-π-1A structure yielded a relevant increase of the DSSC efficiency up to about 8% [33].

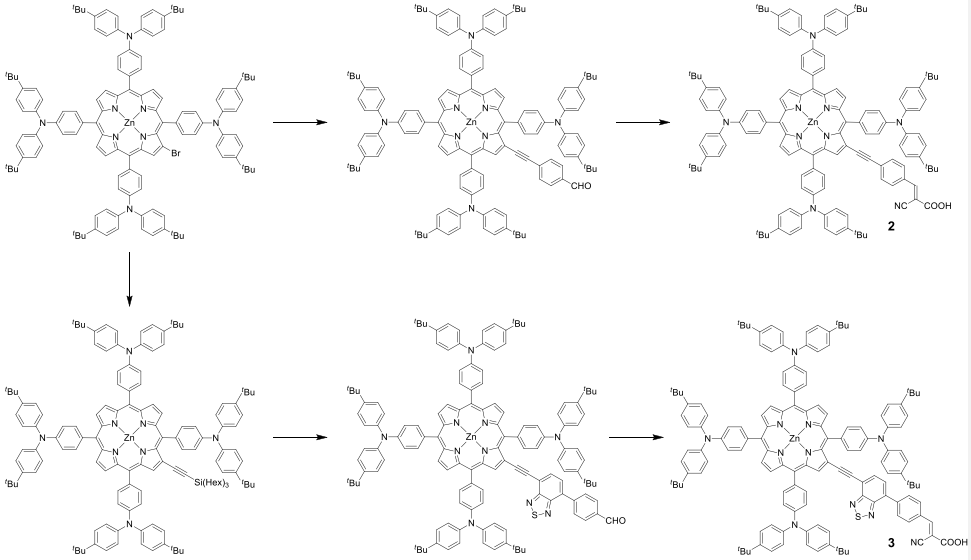


**Scheme 5**. Synthesis of 4D-π-1A type green $Zn^{II}$ porphyrins **2** and **3**.

In conclusion well-engineered and sterically simple β substituted porphyrinic dyes can be obtained by few reaction steps and with efficient synthetic procedures. A rational tailoring of the porphyrinic structure allows to tune their electronic and photoelectrochemical properties in order to reach good conversion efficiencies thus making the β-substituted $Zn^{II}$ tetraarylporphyrins promising for a scale up of the production of valuable dyes for DSSC.

### 3. β substituted metal porphyrins

The relevant properties to be considered in the design of dyes for DSSCs are the molecular orbitals energy and the HOMO-LUMO gap, the extension and intensity of the electronic absorptions and finally the molecular structure which may affect the aggregation states of the dye, when adsorbed on the surface of the $TiO_2$ photoanode. In tetraaryl metal porphyrins dyes, substitution at the β pyrrolic position was reported to exert more severe steric effects with respect to that at the *meso* positions, leading to a larger distortion of the macrocycle, resulting in a red shift in the absorption spectra and reducing the aggregation effects [58-60]. Electrochemical investigations indicate that the porphyrin ring oxidation is more facile for β-substituted porphyrins than for *meso*-substituted analogues [61]. This was in part attributed to the electron rich nature of the β-position of the tetraaryl porphyrin ring [62], while in *meso* diaryl substituted push-pull porphyrins, the pseudo quinoid proposed electronic structure is origin of the quite different electrochemical properties resulting from the push-pull arrangement [63].

### *3.1. Tetraaryl β substituted $Zn^{II}$ porphyrins*

Kay and Grätzel in their pioneering work published in 1993 [64], reported the first example of a DSSC based on a $Zn^{II}$ porphyrin substituted in β pyrrolic position with efficiency η= 2.6%, when DSSC based on Ru complexes had reached already about 10% efficiency [17].

In 2004 Grätzel, Nazeeruddin et al. [65] developed a family of β substituted metal porphyrins with different central metal ions ($Cu^{II}$ or $Zn^{II}$ ) and with two kinds of anchoring groups (COOH or $PO_3H_2$) concluding that the $Zn^{II}$ porphyrin **4,** with a carboxylic anchoring group, was the most performing with 4.8 % efficiency (Figure 4). In 2005 the same authors [66] reported on a series of new green $Zn^{II}$ tetraphenyl porphyrins substituted in β pyrrolic position with a π delocalised organic pendant carrying a cyanoacrylic anchoring group. Among the different $Zn^{II}$ porphyrins investigated, the green dye **5** in the presence of chenodehoxycolic acid (CDCA) reached a 5.6 % efficiency and the dark green dye **6** reached a 4% efficiency (Figure 4).

As discussed later in detail in Section 4, DFT calculations have shown that, comparing with the reference unsubstituted $Zn^{II}$ tetraarylporphyrin (ZnTPP), the presence of electron withdrawing groups on the β substituent modulates the absorption spectrum stabilizing the energies of the LUMO and LUMO+2 orbitals, with an extension of these orbitals onto the β substituent which implies an increased tendency of electron transfer from the porphyrinic core to the β substituent and consequently to the $TiO_2$ surface [66].

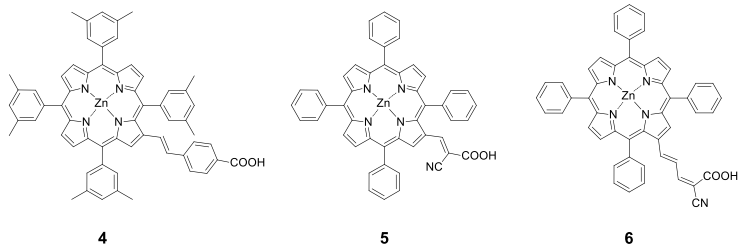


**4** **5** **6**

**Figure 4**. Molecular structures of **4** (η=4.8%), **5** (η=5.6%) green, **6** (η=4.0%) dark green

Later the same authors synthesized a series of green tetraaryl $Zn^{II}$ porphyrins showing incident photon to current conversion efficiency (IPCE) values up to 75% and power conversion efficiencies from 5.1% to 7.1%. The dye **1**, showing the best efficiency of η=7.1 % is reported in Figure 3 [30].

Later Arai, Segawa et al. [67] reported a series of tetraphenyl $Zn^{II}$ porphyrins with one or two acetylenic functional groups at the β pyrrolic position (Figure 5). The green doubly substituted $Zn^{II}$ porphyrin **11** leads, in the presence of coadsorbate chenodeoxycholic acid (CDCA) to a near unity IPCE value, surpassing IPCE maxima of the purple mono substituted derivative. In accordance the double substitution leads to higher overall efficiency (5.7%) with respect to the various monosubstitutions (Figure 5).

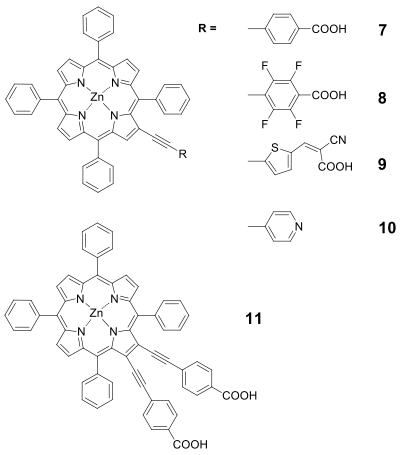


**Figure 5.** Molecular structures of **7** (η=4.9%) purple, **8** (η=4.5%) purple, **9** (η=4.6%) purple, **10** (η=4.0%) purple, **11** (η= 5.7%) green

A comparative investigation on tetraaryl β monosubstituted and 5,15 *meso* push-pull disubstituted diaryl $Zn^{II}$ porphyrins has been carried out by Pizzotti *el al.* [24] in order to compare their performances in DSSCs (Figure 6). Although the HOMO-LUMO energy gap of the push-pull *meso*-disubstituted porphyrins is narrower, thus allowing an easier charge transfer along the push-pull system, the β mono substituted dyes show comparable or even better DSSC efficiencies.

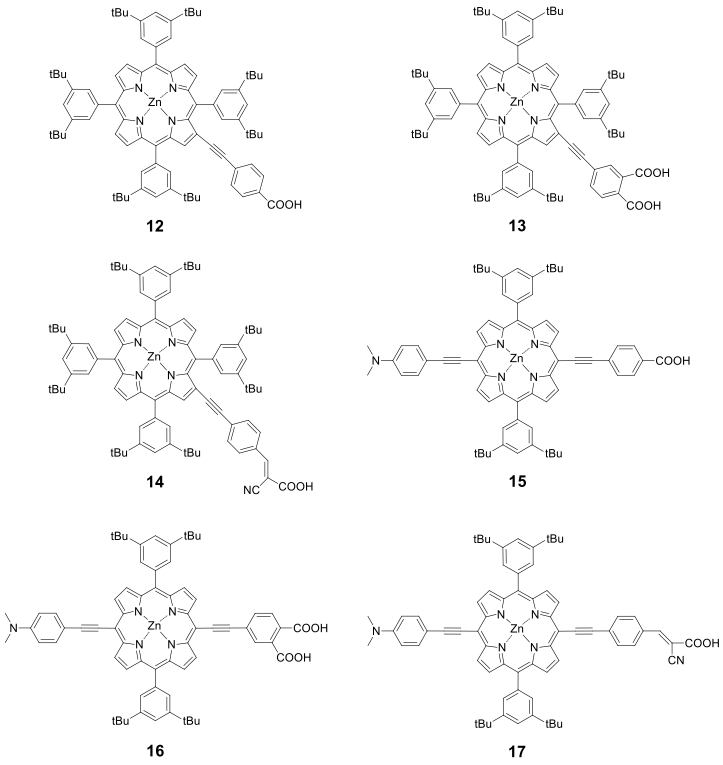


**Figure 6**. Molecular structures of **12** (η= 3.1%) green, **13** (η= 4.0) green-red, **14** (η=4.6% improved to 6.1% [68]) green-red, **15** (η= 3.9%) green, **16** ( η=3.0%) green, **17** (η =4.2%) green

This behavior was attributed, in first approximation, to a more facile charge injection into the photoanode, as suggested by the electron distribution obtained by DFT calculations of a simple model of a β monosubstituted $Zn^{II}$ porphyrinic dye interacting with the $TiO_2$ surface [24]. In agreement with these findings, IPCE spectra of β substituted $Zn^{II}$ porphyrinic dyes show more intense values over the range 350-650 nm compared to those of *meso* substituted ones which produce IPCE spectra with two well separated less intense peaks, strictly corresponding to B and Q absorption bands of the push-pull system (Figure 7).

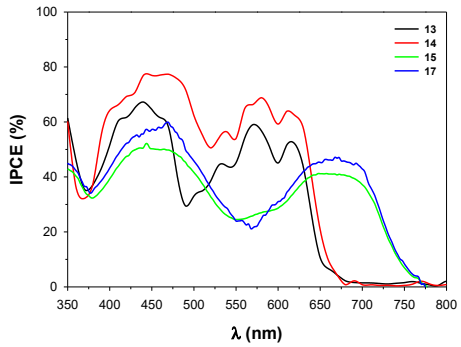


**Figure 7**. IPCE spectra of β-substituted $Zn^{II}$ porphyrinic dyes **13** and **14** compared to those of *meso* substituted **15** and **17** [24].

By combining time-resolved spectroscopy with photophysical and photoelectrochemical techniques on dyes **14** and **17**, Di Carlo, Caramori *et al.* [68] have recently reported (as discussed in detail in Section **5**.) that the origin of the better performance of DSSC based on **14** with respect to **17**, depends on a significant reduction of the recombination rate with the redox iodine based mediator rather than on charge injection yield.

A similar comparison on the *meso* and β substituted $Zn^{II}$ porphyrins reported in Figure 8 has been carried out by Giribabu *et al.* [69] confirming that the β substituted $Zn^{II}$ porphyrins **18** and **19**, are characterized by rather low efficiencies, but higher than the corresponding *meso* disubstituted **20** and **21**.

In conclusion both these two comparative investigations have evidenced that the well diffused paradigm supporting that 5,15 push-pull disubstituted *meso* $Zn^{II}$ porphyrins lead to the best DSSC efficiencies, is not so convincing.

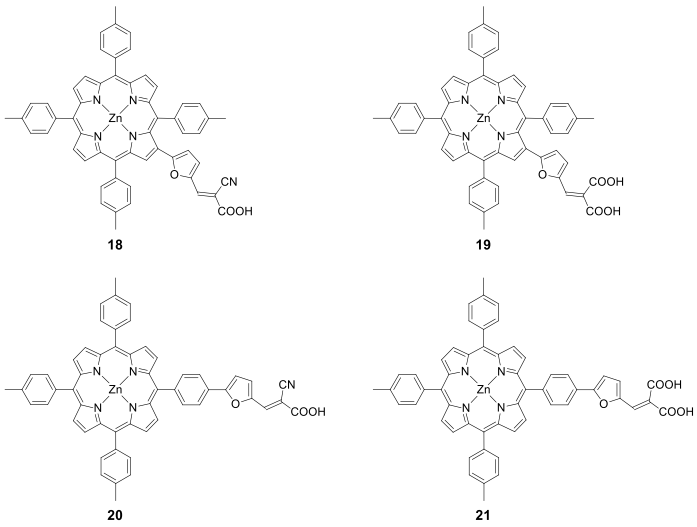


**Figure 8.** Molecular structures of **18** (η= 0.13%) brown, **19** (η= 0.10%), **20** (η= 0.11%), **21** (η = 0.0013%)

*3.2. Tetraaryl β substituted $Zn^{II}$ porphyrins with anti-aggregation substituents*

Large molecules with an extended pseudo planar π-system like porphyrins are known to be affected by a high tendency to aggregate due to π–π staking interactions [70]. This aspect is detrimental when $Zn^{II}$ porphyrins are used as dyes in DSSC. In fact the formation of dye-aggregates on the surface of the mesoporous semiconductor photoanode ($TiO_2$) results in a significant decrease of the electron injection efficiency [71]. Moreover, porphyrinic dyes presented photovoltaic characteristics with lower $V_{OC}$ values than that registered for the ruthenium dyes like N719 [34], even in the case of meso-disubstituted push-pull architectures featured by great light-harvesting ability and good performance.

The more facile charge recombination between the electron injected into the photoanode and the reducing component of the redox shuttle could be the possible origin of such low $V_{OC}$ values [4, 6, 34, 72]. In fact the almost flat porphyrinic structure cannot produce a substantial three-dimensional

barrier on the $TiO_2$ surface necessary to prevent a significant contact and an easy electron exchange process between the photoanode surface and the electrolyte.

At the same time, a shorter electron lifetime with respect to N719 dye was reported [73], supported by the evidence of a coordination process of the basic $I_3^-$ species on the acidic $Zn^{II}$ metal centre of the porphyrinic ring adsorbed on the $TiO_2$ surface, thus allowing, due to the close proximity of the reducing $I_3^-$ species to the photoanode surface, a faster recombination with the injected electron [36, 73].

Coadsorbates like CDCA have been used to brake off the porphyrinic aggregates on the $TiO_2$ surface, but in the same time a lower dye-loading is produced, with a consequent decrease of $J_{SC}$ values and of the overall efficiency of the DSSC. This aggregation process can be hindered by introduction of bulky groups like *tert*-butyl linked to the *meta* positions of phenyl rings on the *meso* positions of the porphyrinic dyes (see **22** in Figure 9). The higher $J_{SC}$ values with an overall improvement of the power conversion efficiencies, confirmed a positive effect of such kind of steric hindrance in preventing aggregation [71].

Another structural approach based on steric hindrance effects was developed by introduction of long alkoxy chains, for instance at the *ortho* position of the two opposite phenyl rings of the 5,15 push-pull *meso*-disubstituted $Zn^{II}$ diarylporphyrins (see **23** in Figure 9). The peculiar position of these chains produces over both the porphyrinic faces a steric congestion thus reducing aggregation and in the same time shielding the $Zn^{II}$ metal centre from the possible coordination of the $I_3^-$ ion. An improvement of conversion efficiency to about 9 % was achieved, when *ortho* dodecoxy chains (**23**, $\eta$= 10.2 %) instead of *tert*-butyl groups linked at the *meta* positions (**22**, $\eta$= 9.34 %) have been introduced in the two phenyl rings [28].

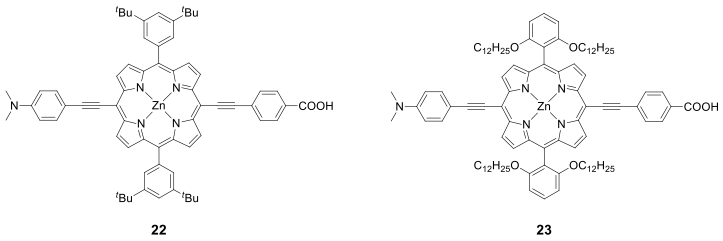


**Figure 9.** Molecular structures of **22** and **23**

Applying to the push-pull porphyrinic dye **YD2** (η=11% in presence of CDCA) [27] the same structural strategy, the new dye **YD2-oC8** (see Figure 2) was obtained, reaching a power conversion efficiency over 12 % when it was co-sensitized with the organic dye **Y123** and when a $Co^{III}/Co^{II}$-based redox electrolyte was used [21]. Since the cationic Co-based shuttle is a highly charge-recombinant redox electrolyte, the increase of conversion efficiency is clearly due to an efficient aliphatic barrier at the photoanode against charge recombination. Today, this structural strategy is considered a milestone for achieving top performances, even without the introduction of a co-sensitizer [22]. This strategy has been thus extended by some of us to β substituted tetraaryl $Zn^{II}$ porphyrinic dyes [24], with the synthesis of three β-substituted tetraaryl $Zn^{II}$ porphyrins bearing octyloxy chains at the *ortho,ortho-* (*o,o-*), *ortho,para-* (*o,p-*), or *ortho*-positions (*o-*) of the four phenyl groups (**24, 25** and **26** respectively) (Figure 10) [32].

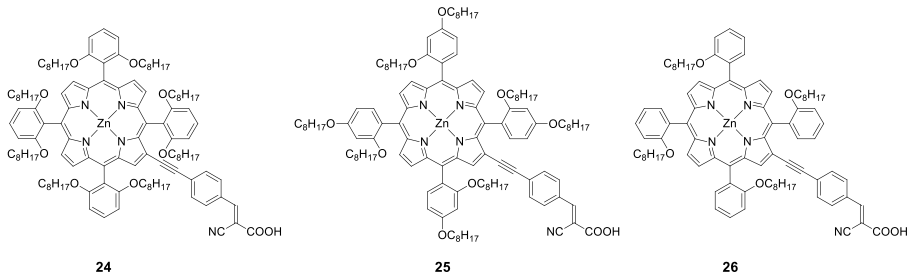

**Figure 10.** Molecular structures of **24** (η=5.2%) pale green, **25** (η=4.7%) purple, **26** (η= 6.1%) purple

The introduction of these alkoxy chains and in particular their position on the phenyl rings, leads to an impressive improvement of their DSSC PV performance with respect to the 3.4 % of the reference dye **14** (see Figure 6), working under the same experimental conditions. The *o*- or *o,p*-substitution of the phenyl rings as in **25** and **26** produces an electronic absorption spectrum comparable to that of the reference dye **14**, but the HOMO-LUMO gap is slightly increased up to 2.10, 2.11 eV respectively. In particular the LUMO level results higher than that of **14** as it occurs when **22** and **23** in Figure 9 are compared [28].

However the *o,o*-substitution produces the most relevant effect on the electronic structure of **24**, with a significant red-shift of its Q absorption bands and a narrow electrochemical HOMO-LUMO energy gap of only 1.77 eV, surprisingly comparable to that usually reported for 5,15 push-pull *meso* disubstituted diaryl $Zn^{II}$ porphyrinic dyes [25, 74].

The power conversion efficiencies attained by using **24**, **25** and **26** as dyes in DSSCs were found to be 5.2%, 4.7% and 6.1%, respectively, showing for the latter an increase of almost 80% in performance when compared to the reference dye **14**, working under the same experimental conditions. The large increase of $J_{SC}$ when **26** is the dye (11.8 $mAcm^{-2}$) is mainly in charge of this relevant performance, although also the $V_{OC}$ value (694 mV) is the best observed up to now for DSSC based on this kind of β-substituted $Zn^{II}$ tetraarylporphyrins [32].

It is worth pointing out that an increase of 80% of the power conversion is a relevant effect, taking into consideration that the strategy of increasing steric hindrance, when applied to 5,15 push-pull *meso* disubstituted diaryl $Zn^{II}$ porphyrins, produces an increase of the power efficiency of only 10% as when **22** and **23** of Figure 9 are compared [28].

The presence of eight alkoxy chains turns the porphyrinic structures to be a sort of hydrophobic spheres, difficult to be absorbed on the hydrophilic surface of $TiO_2$, so that addition of CDCA was

necessary to make the $TiO_2$ surface a more lipophilic environment, in order to allow enough dye loading. Therefore a high amount of CDCA (10 times more than that of the dye) was necessary to optimize the power conversion, thus producing a surface concentration of **24** and **25** about half of that of **26**. These evidences confirm that the presence of a single long alkoxy chain in the *o*-position allows dye **26** to pack more favorably on the $TiO_2$ surface producing a better loading of the dye on the photoanode but in the same time a shift of the color from pale green as **24** to purple as **26**.

Starting from these evidences and to optimize the performance of **26**, the effect of the length and nature of different alkoxy chains linked to only one *ortho* position of the four aromatic rings was investigated as well, giving particular attention to aggregation effects and light harvesting capability of the dyes (Figure 11) [56].

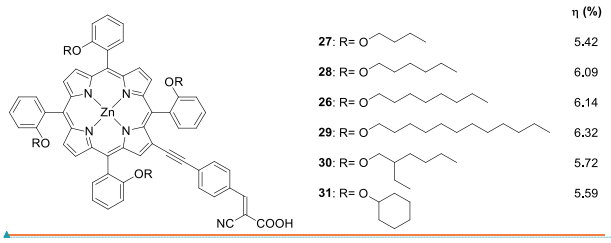


**Figure 11.** Molecular structures of red dyes investigated in ref. [56].

As expected, the different alkoxy chains do not perturb the electronic properties of the dyes: the electronic absorption spectra are almost superimposable and only very small differences from the electrochemical point of view were found. However the photovoltaic characteristics of the DSSCs based on this series reveal an almost linear relationship between the power conversion efficiency and the alkoxy chain length both in the presence or in the absence of a disaggregating agent like CDCA. In particular, the best PCE obtained, working with an amount of CDCA five times higher than that of the dye, linearly increases with the length of the alkoxy chain due to a remarkable increase of $J_{SC}$ and $V_{OC}$ values passing from dye **27** (12 mA $cm^{-2}$, 645 mV) to dye **29** (13.2 mA $cm^{-2}$, 705 mV). These experimental evidences confirm that longer alkoxy chains provide



Codice campo modificato

to better DSSC performaces as a result of a better enveloping of the porphyrininc core, producing a significant anti-aggregation and photoanode-shielding effect.

In particular also the charge injection process into the photoanode appears to be influenced by the molecular architecture imposed by the alkoxy substituent, because time-correlated single photon counting analysis of dye-sensitized $Al_2O_3$ films obtained from CDCA-free solutions, has shown that the presence of longer alkyl chains increases the charge injection properties, in fact the dye excited state deactivation follows this trend: **29** > **28** > **30** > **31** nicely in agreement with the increase of the length of the alkoxy chain [56]. It appears thus that the length of the alkoxy chain in *ortho* position of the phenyl substituents seriously impacts the intermolecular charge-transfer processes, affected by the dye-to-dye interaction through a reduction of the self-quenching phenomena, and by a diminishing of the back electron transfer rate from $TiO_2$ to the electrolyte, due to an increase of the enveloping protective effect of the long alkoxy chain in *ortho* position.

### *3.3. Tetraaryl β pyrrolic monosubstituted $Zn^{II}$ porphyrins with panchromatic effect.*

The limited performances of $Zn^{II}$ porphyrins as dyes for DSSC could be attributed to their limited solar light harvesting, particularly in the range 450-550 nm. In fact IPCE spectra of $Zn^{II}$ porphyrinic dyes generally show two quite strong well separated peaks corresponding to B and Q absorption bands, with a region of low intensity between 450 and 550 nm. A strategy to overcome this limitation was the introduction of the (E)-dithienylethylene (DTE) unit, which strongly absorbs in this specific range, in a β π delocalized chain connecting the porphyrinic ring and the carboxylic anchoring group as reported by Ko and Lee [75] for β substituted tetraaryl $Zn^{II}$ porphyrins, by Bisquert, Langa et al. [76] for *meso* substituted triaryl $Zn^{II}$ porphyrins, and confirmed as a general strategy by other authors [77].

This panchromatic strategy has been recently extended by Pizzotti et al. [31] to $Zn^{II}$ tetraaryl porphyrins β substituted with a π delocalized chain carrying the cyanoacrylic anchoring group, and

containing two thienylic units (Figure 12). Even if this highly π delocalized chain produces a significant panchromatic effect in the electronic absorption spectrum in the range 430-650 nm and intense and homogeneous IPCE spectra in the range 400-650 nm for the three red dyes **32-34** (Figure 13), the increase of power efficiency η is still quite limited, reaching values between 4.3 and 5.2%. Moreover DFT theoretical calculations have demonstrated that the power efficiency may be dependent on the nature of the π spacer connecting the DTE units with the porphyrinic ring (Figure 13). In fact its nature affects the linearity and planarity of the structure of the dye which seems to be the origin of the better performance of dye **32** in DSSC.

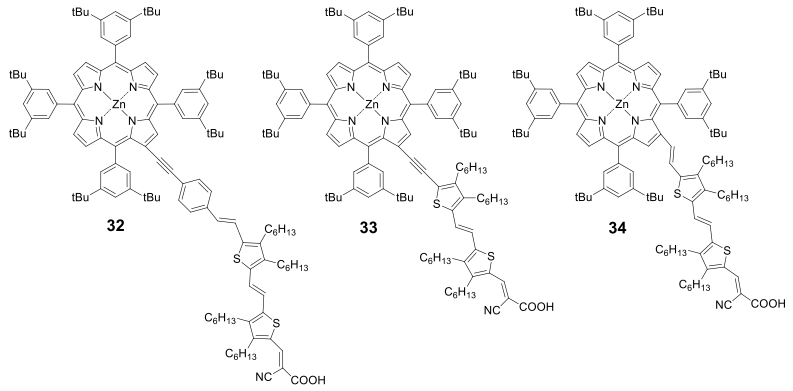


**Figure 12.** Molecular structures of **32** (η=5.2%) purple, **33** (η=4.7%) purple, and **34** (η=4.3%) purple.

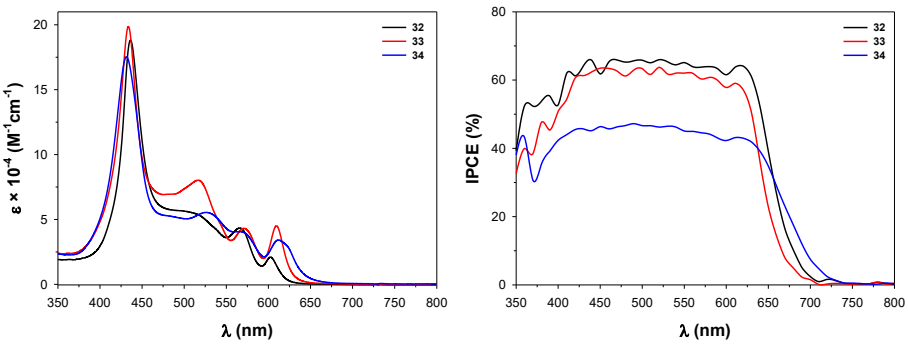


**Figure 13**. Electronic absorption spectra and IPCE spectra of **32-34**.

More recently Zhao, Zhang et al. [78] reported similar panchromatic effects by introduction of two electron deficient units DPQ (**36**) and BTD (**37**) in the π linker at the β position of 5,10,15,20 tetraphenyl $Zn^{II}$ porphyrin (Figure 14). DFT calculation have shown that, compared with the reference dye **35**, the LUMO energy level is decreased for both **36** and **37**, resulting in broader absorption spectra and improved IPCE values in the range 350-500 nm (particularly for **37**), ensuring a better light harvesting property and, in the latter case, a better DSSC performance.

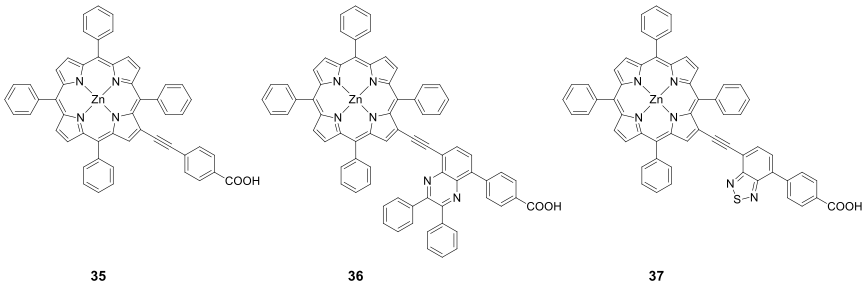


**Figure 14.** Molecular structures of **35** (η= 4.02%) purple, **36** (η=4.47%) purple and **37** (η= 6.14%) purple

However it must be pointed out that the introduction, in β position, of substituents with a significant panchromatic effect, gives place to a purple color of the dyes, thus limiting their potential application in DSSC to be used for smart windows.

*3.4. Unconventional push-pull $Zn^{II}$ porphyrins*

An attractive design feature involves the presence of two separate acid anchoring groups, π conjugated to the porphyrin ring. If they are located on the same side of the porphyrin core at the β positions, no problem arising from the steric hindrance would be expected [79]. In this contest Kim and coworkers synthesized three new green push-pull β functionalized $Zn^{II}$ porphyrins with a diaryl amine as electron donating group in *meso* position [80]. The best performance was reached by the $Zn^{II}$ porphyrin **40** with η=7.5 % (Figure 15), more recently improved by the same authors to η=8.2% by using the $Co^{III}/Co^{II}$ tris-bipyridyl couple as redox mediator [50].

This work evidences that the flexible and small alkenyl π conjugated spacer plays a critical role in effective electronic coupling between the porphyrin core and the anchoring groups and in controlling the dye geometries and the dye loading on the $TiO_2$ surface, with suppression of dye aggregation in comparison to those of other aryl substituted porphyrinic dyes such as **41**, **42** and **43**, **44** [50].

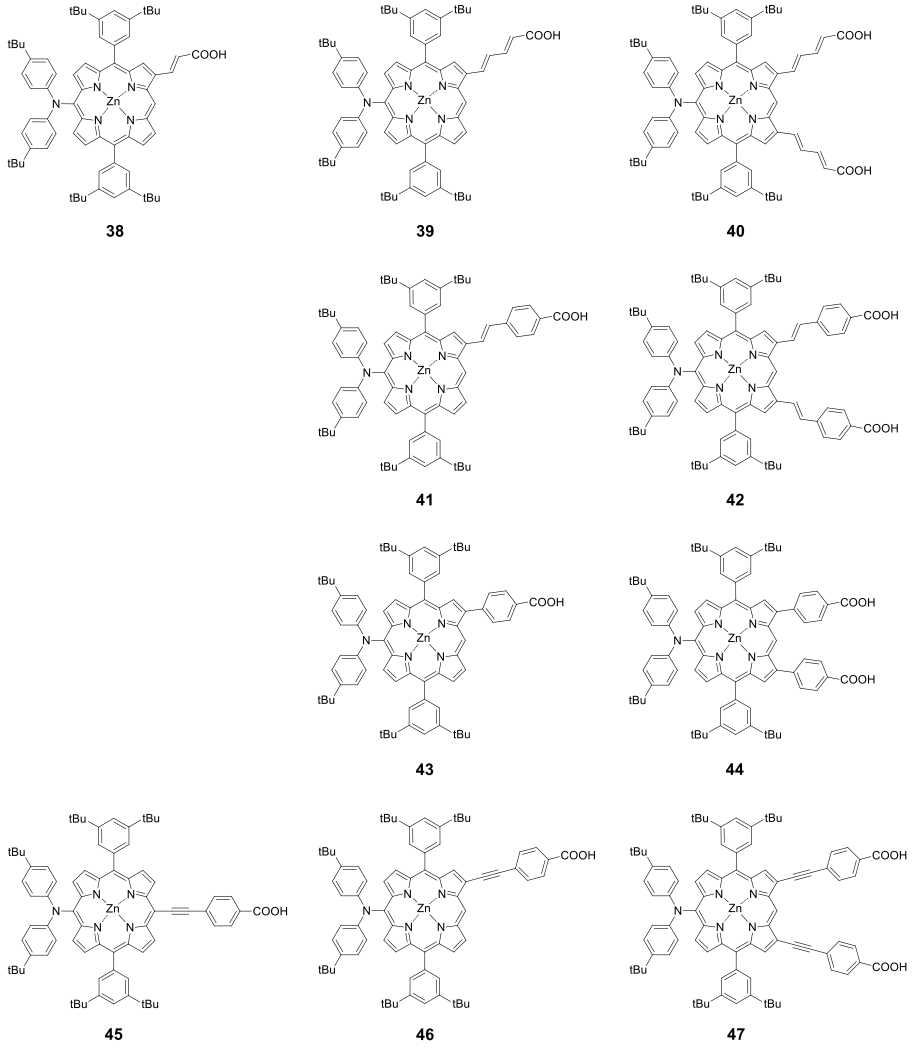


**Figure 15.** Chemical structures of dyes reported in Ref. [80], [50] and [51].

An investigation on the effect of the nature of the π conjugated spacer on the performance of the DSSCs, carried out on four new $Zn^{II}$ porphyrins [50] (Figure 15) has confirmed that a β-ethenyl phenyl spacer allows a better electronic interaction of the carboxylic anchoring group with the porphyrinic core than a simple phenyl spacer. In fact the photovoltaic performance of DSSCs

sensitized by $Zn^{II}$ porpyrins such as **41** and **42** exhibit higher power conversion efficiency than those involving $Zn^{II}$ porphyrins like **43** and **44** (Figure 15). In all cases the $Co^{III}/Co^{II}$ based mediator produces an increase in η performance with respect to the $I^-/I_3^-$mediator.

When the linker is a π ethynyl phenyl system instead of a π ethenyl phenyl one as in **46** and **47** (Figure 15), the photophysical and electrochemical properties are similar to those of the *meso* disubstituted reference dye **45**, with a power conversion efficiency of the β monosubstituted dye **46** superior to that of the disubstituted **47** and similar to that of **45** [51].

As previously reported, in order to obtain the new 2,12 β disubstituted porphyrins, reported in Figure 16, Di Carlo et al. [46] have optimized the synthesis of a 5,10,15,20-tetra(3,5 di-*tert*-butylphenyl)porphyrin with two bromine atoms in 2,12 β-pyrrolic position, obtained by a light induced selective reaction. The position of the two bromine atoms in the porphyrinic ring was confirmed by the X ray structure of the $Ni^{II}$ complex, determined with unprecedented probability levels [46].

The performances of the DSSCs based on β disubstituted green 2,12 push-pull dyes **48** and **49** (Figure 16) were found to be slightly superior to those of DSSCs based on the β monosubstituted dyes **12** and **14**, respectively, and also superior to that of the corresponding 5,15 *meso*-disubstituted push pull dyes **15** and **17**, reported in Figure 6 [24].

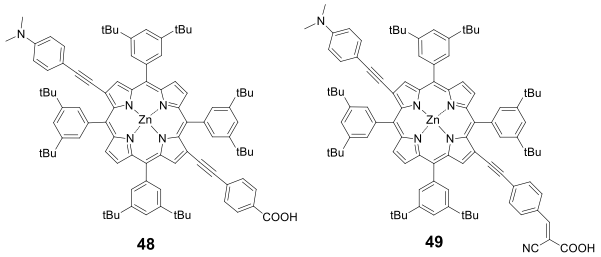


**Figure 16.** Molecular structures of **48** (η=4.1%) green and **49** (η= 4.7%) green.

The higher efficiency of β disubstituted 2,12 push-pull $Zn^{II}$ porphyrins with respect to the corresponding 5,15 *meso* push-pull disubstituted is quite unexpected because electron transfer by excitation along the push-pull system was found to be more efficient through the 5,15 *meso* positions. However the IPCE spectra of both β mono or disubstituted porphyrinic dyes **12**, **14**, **48**, **49** are more diffuse and intense over the wavelength range 350-650nm with respect to the *meso* disubstituted porphyrinic dyes **15** and **17**. In this latter species the IPCE spectra show two well separated and less intense peaks, corresponding to B and Q adsorption bands, with weak values in the mid-range (530-610 nm). It must be pointed out that the β $Zn^{II}$ porphyrins **48** and **49** are less flat than the corresponding *meso* disubstituted **15** and **17** producing less recombination effects with the photoanode due to more bulky and sterically hindered structures.

Recent advances in designing push-pull systems on the opposed pyrrolic positions of the porphyrinic core have been also achieved by Imahori [53] and Wang [54, 55] (Figure 17). The former evaluated the effect on PV properties of a donor-acceptor system bearing an electron-donating triarylamino group at the β,β'-edge through a fused imidazole group and an electron-withdrawing carboxyquinoxalino anchoring group at the opposite β,β'-edge, while the push-pull effect on a series of β-functionalized dibenzoporphyrins has been electrochemically, spectroscopically and photo-physically investigated by the latter.

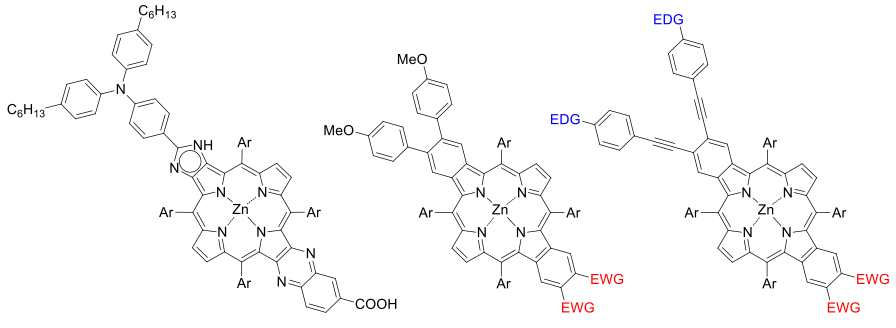


**50** **51** **52**

EWG = -CN, -COOMe, Imide, Pyridyl
EDG = -Phenyl, dimethylaminophenyl

**Figure 17**. Molecular structures of **50** (η=6.8 %), **51** (green) and **52**

With the aim to further enhance the donor-acceptor character and to improve the light collection efficiency of tetraarylporphyrin dyes having a β-substitution pattern, the new 4D-π-1A type push-pull system has been developed very recently. In particular two novel green porphyrins, **2** and **3**, (Scheme 5), with an increased charge-separation character and featured by extended electron absorption across the visible spectrum have been obtained by accessible and efficient synthetic pathways. The four arylamino donor substituents in *meso* positions and an acceptor pendant in β-position have shown to strongly narrow the HOMO-LUMO energy gap (as discussed in detail in section **4**.) improving the light-collection efficiency of the dyes both in the visible and NIR regions[33]. The key features of *meso*- and β-substituted porphyrins have been merged in such a new structural architecture in order to guarantee ideal characteristics for BIPV application.

*3.5. Fused porphyrinic and polyporphyrinic systems involving β substitution.*

Another strategy to fill the absorption region between the B and Q bands and to shift in the same time to NIR the absorption spectrum of a porphyrinic system, thus improving the light harvesting ability, is to extend the π system by fusing aromatic rings with the porphyrinic core. The extension of π conjugation reduces the HOMO-LUMO gap, resulting in broadening and red shift of the absorption and increasing intensity of the Q bands. In 2007 Imahori et al. [81, 82] reported the first green *meso*-β-edge fused $Zn^{II}$ porphyrin characterized by a DSSC with 4.1% efficiency with 50% increase with respect the structurally related unfused $Zn^{II}$ porphyrin. The same authors reported in 2008 the dark red β,β'- edge fused $Zn^{II}$ porphyrin **55**, involving a quinoxaline fused bridge which, under optimized conditions, reaches a conversion efficiency of 6.3 % (Figure 18) [53, 83-86].

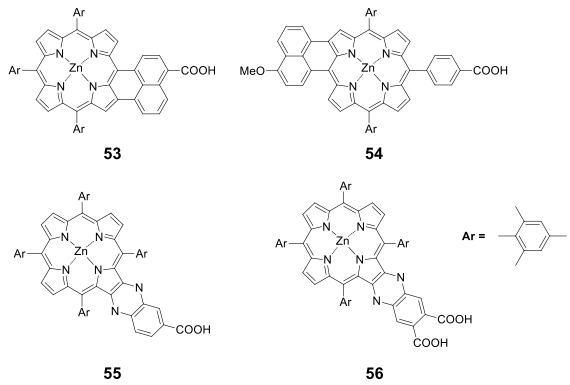


**Figure 18**. Molecular structures of $Zn^{II}$ porphyrins **53** (η= 4.1%) green, **54** (η= 1.1%) green, **55** (η= 6.3%) dark red and **56** (η= 4.0%) dark red.

Wang, Wu and coworkers reported a new strategy by designing dyes **58** and **59** (Figure 19) with significant absorptions in the NIR by fusing an electron rich $Zn^{II}$ porphyrin to the π system of the perylene anhydride [87]. The IPCE spectra of their DSSC covered the entire visibile range extending into the NIR region up to 1000 nm, which is very impressive for this kind of dyes. However these highly fused and planar dyes displayed moderate power conversion efficiencies as expected for IPCE values about 30% due to strong aggregation and a too low energy level of LUMO excited state, so producing a low charge injection into the $TiO_2$ photoanode. In fact narrowing the HOMO-LUMO gap, the LUMO level of the $TiO_2$ conduction band becomes too close to the LUMO level of the dye with reduction of the energetic driving force necessary for charge injection, so producing very low DSSC efficiency (Figure 19).

A similar problem was reported by Anderson, Snaith et al. for the antracene-fused porphyrinic dye **57**, characterized by a very strong red-shift and broadening of the absorption spectrum to about 1000 nm (Figure 19) [88].

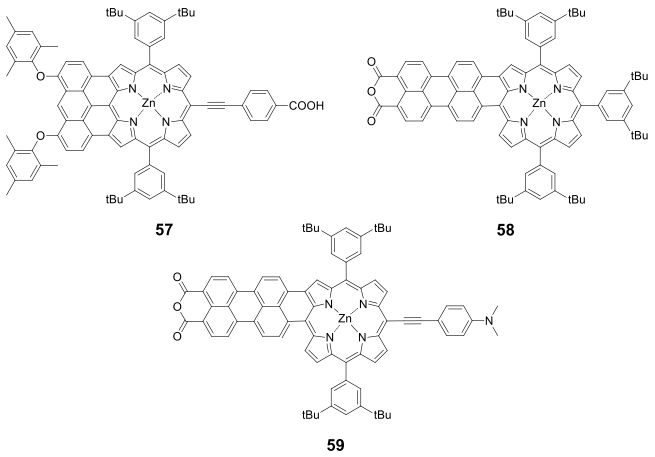


**Figure 19.** Molecular structures of polycyclic fused $Zn^{II}$ porphyrins **57** (η about 0.05%) black, **58** (η= 1.26%) red, **59** (η= 1.36%) red.

Diau, Yeh et al. synthesized the triply fused YDD2 and the doubly fused YDD3 $Zn^{II}$ porphyrinic systems which showed very low DSSC performance for similar reasons [89]. In fact the HOMO-LUMO gap is so narrow that, for instance in the case of the triply fused system **60**, the electron injection is essentially forbidden, being the LUMO energy level lower than the conduction band of $TiO_2$. Only for the doubly fused system **61,** a small response is observed in the IPCE spectrum (Figure 20).

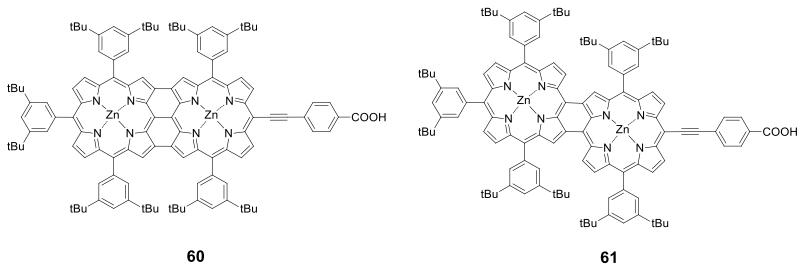


**Figure 20.** Molecular structures of fused $Zn^{II}$ porphyrin dimers **60** and **61**

In conclusion, despite their extended light harvesting and their strong NIR adsorption, the DSSC efficiency of these panchromatic $Zn^{II}$ porphyrins is generally low.

Another strategy to increase the light harvesting of the β substituted $Zn^{II}$ porphyrinic dyes could be the linking of two or more porphyrin cores through their *meso* positions. . Following this approach, in 2009 Kim, Osuka et al. [90] reported a series of doubly β functionalized $Zn^{II}$ porphyrin dimers (Figure 21).

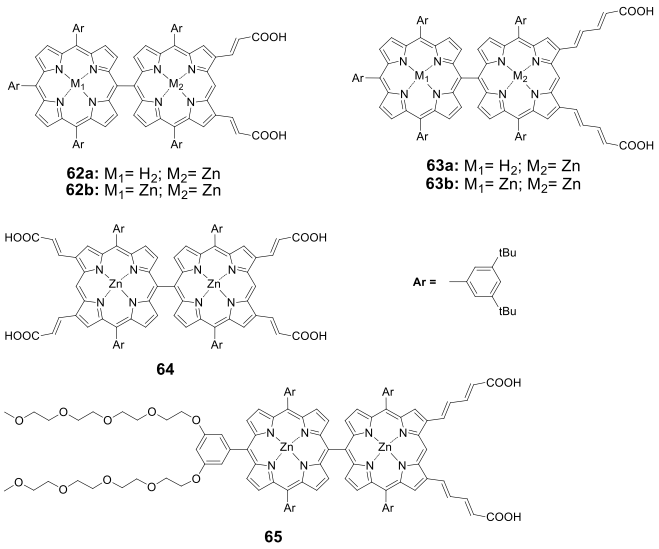


**Figure 21.** Molecular structures of polyporphyrinic systems.

The highest conversion efficiency was reported for **65** with η= 4.2 %, suggesting that the increased spectral extension, obtained by direct linkage of two porphyrinic cores, can harvest a broad range of solar spectrum, thus favoring a significant DSSC efficiency. Therefore this could be an effective strategy for a rational design of efficient porphyrinic dyes for DSSCs.

## 4. Electronic structures, absorption spectra and charge transfer processes

Many theoretical papers, mainly based on DFT-TDDFT calculations, have been published aimed to investigate the effect of β substitution on the electronic structure and on the origin of the electronic absorption spectra of porphyrin dyes with particular reference to charge transfer processes controlled by the nature of various substituents in β position [24, 31, 91-97]. Such charge transfer processes, which generate charge separation, are originated, in DSSCs, by the flow of electrons from the dye to the $TiO_2$ photoanode.

In general DFT calculations have shown that β substitution generates a perturbation of the classical four frontier molecular orbitals (2 HOMO and 2 LUMO) of the Gouterman's four orbital model [95, 96] of the porphyrinic electronic structure, whose energy and electron density can be tuned acting on the nature of the β substituent.

Already in the pioneering works of Gordon et al. [91, 92] it was shown that substitution at the β position with a π delocalized acceptor substituent does not affect markedly the relative energies of the two nearly degenerate HOMO orbitals still centered on the porphyrinic ring, but the degeneracy of the two LUMO is broken with parallel decrease of the HOMO-LUMO energy gap.
Moreover when the β substituent is based on an ethynylphenyl π linker bearing a carboxylic or a cyanoacrylic acid group, the splitting of the LUMO and LUMO+1 energy levels increases in the latter case due to a significant decrease of the LUMO energy with parallel decrease of the HOMO-LUMO energy gap as in **12** and **14** (Figure 22) [24, 31], and an increased localization of electron density on the β substituent [24]. In the same time the LUMO+2, which is far away in energy from the two degenerate LUMO levels in the Gouterman model, becomes closer in energy to LUMO+1, thus giving place to a nearly degenerate LUMO+1 and LUMO+2 system. Such relevant perturbation of the LUMO levels is due to a significant electron density on the β substituent induced by the electron withdrawing properties of the cyanoacrylic acid [24]. A similar departure from the Gouterman model was also reported for a series of other β substituted $Zn^{II}$ porphyrins.[97]

Such perturbation of the Gouterman model is due to an internal push-pull system of the porphyrinic electronic structure, with the donor part mainly centered on the porphyrinic core (HOMO and HOMO-1 orbitals) and the acceptor one mainly localized on the β ethynylphenyl substituent (LUMO and LUMO+2 orbitals). As a consequence the HOMO-LUMO and HOMO-LUMO+2 electronic transitions are associated with an electron transfer from the "push" porphyrinic core to the "pull" β substituent (Figure 22), producing charge separations with significant shift of the electron density on the anchoring carboxylic group at the end of the β substituent.

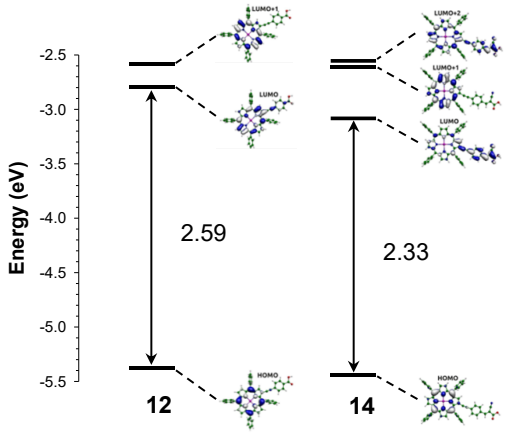


**Figure 22.** Energy levels and isodensity plots of the HOMO, LUMO and LUMO+1 (dye **12**) or HOMO, LUMO, LUMO+1 and LUMO+2 (dye **14**) mainly involved in the electron transfer processes.

In general, for a series of $Zn^{II}$ tetraaryl porphyrins with various π delocalized β substituents [92], the HOMO, HOMO-1 and LUMO+1 levels are characterized by an electron density centered on the porphyrinic ring, while the electron density of the LUMO, LUMO+2 and HOMO-2 orbitals is mainly localized on the β substituent. Such push-pull asymmetry of the electronic structure is more pronounced when the β substituent carries a strong electron withdrawing group such as the cyanoacrylic acid.

These electronic features are well reflected in the electronic absorption spectra. When the β substituent is based on an ethynylphenyl linker carrying an electron withdrawing group as for example a carboxylic group, the electronic absorption spectrum shows a strong and rather broad B band at about 430-460 nm and only two weaker Q bands at about 566-577 and 604-616 nm respectively as for dyes **12** and **48** [24] as expected for a decrease of the microsymmetry as considered in the Gouterman model [95, 96] (Figure 23). Indirect evidence for a departure from such a model is given also by the presence of a red shifted shoulder of the broad B band, when the β substituent carries the strong electron withdrawing cyanoacrylic acid group as for dyes **14** and **49**, a feature first reported by Pizzotti et al. [58] with other strong withdrawing substituents in β position.

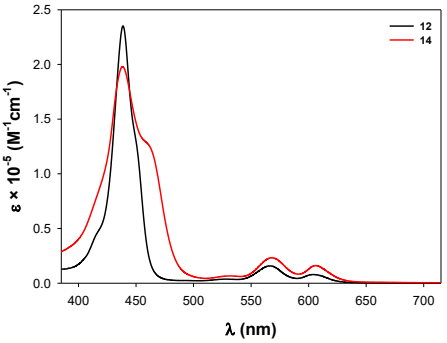


**Figure 23:** Electronic absorption spectra of dyes **12** and **14** respectively with carboxylic and cyanoacrylic terminal group

Of course the charge transfer processes are controlled not only by the nature of the acidic anchoring group of the β substituent, but also by the electronic structure of the π linker connecting the porphyrinic core and the anchoring group, affecting also the energy of LUMO and LUMO+2 (and in some cases of LUMO+3) and consequently the electronic density on the β substituent. [31, 91, 97, 98]. For instance when the linker is a trans butadienic π system (instead of an ethynyl phenyl π system), carrying two carboxylic groups [94] (Figure 24), the electronic transitions involved in

the B and Q bands are quite consistent with the four orbitals Gouterman model [95, 96]. In fact the two Q bands are originated by electronic transitions involving mainly the four HOMO, HOMO-1, LUMO, LUMO+1 frontier orbitals, and also the B band, which is the sum of two bands, is originated by electronic transitions mainly involving the HOMO, HOMO-1, LUMO, LUMO+1 with only a rather partial contribution of the LUMO+2 orbital, not considered in the Gouterman model. It appears thus that the trans butadienic π linker, differently from the ethynyl phenyl linker, does not produce a significant electronic perturbation on the $Zn^{II}$ porphyrinic core, despite the presence of two carboxylic groups on the β substituent.

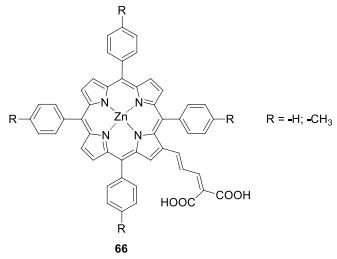


66

**Figure 24**. Molecular structure of **66**

The relevant role of the complexity of the π linker on the energy levels and therefore on the electron transfer transitions, origin of charge transfer processes in β substituted $Zn^{II}$ porphyrinic structures, is well established. For instance it was first emphasized by Gordon et al. [93], who have reported that the presence of a thiophenic chain of increasing length in the π linker of the β substituent, increases the LUMO's splitting. In accordance a longer thiophenic chain induces an increased donor-acceptor character of the electronic structure of the porphyrinic system and consequently a decrease of the HOMO-LUMO energy gap.

Recently some of us [31] have confirmed that by increasing the complexity of π chain of the linker in β position, carrying an anchoring cyanoacrylic acid group, by the introduction of two dithienylethylene moieties (DTE), (see **32-34** in Figure 12) the discrepancy from the Gouterman

model becomes quite relevant. In fact, while the LUMO level is shifted to lower energy with complete break of the degeneracy of LUMO and LUMO+1, and parallel decrease of the HOMO-LUMO energy gap, the energy of both LUMO+2 and LUMO+3, usually much higher, strongly decreases.

At the same time, the energies of the HOMO, HOMO-1 and HOMO-2 levels are not too much affected and their electron density remains still mainly localized on the porphyrinic core and only partially on the DTE units of the π linker. Interestingly the electron density of HOMO-3 level, usually far away in energy, is quite totally localized on the two DTE units and on the π linker (ethenylic or ethynylic). Also in the LUMO level, a significant electron density on the DTE units of the π linker and on the terminal cyanoacrylic acid group is observed, while the LUMO+1 and in particular the LUMO+2 levels still show a relevant electron density on the porphyrinic core [31]. Such electron density distribution is quite different from that typical of β susbstituted $Zn^{II}$ porphyrinic structures involving more simple π linkers [24, 97, 98]. It follows that some electronic charge transfer processes may involve as excited states also the LUMO+3 level, so that the HOMO - LUMO+3 transition, not relevant for other kind of π linkers [24, 97, 98], can give a quite significant contribution to the B band, so that by increasing the complexity of the π linker, the B band may occupy a not trivial role in the generation of significant charge separation by photoexcitation.

The introduction, on a classical push-pull system involving the pyrrolic 2,12 positions, of two ethynylphenyl substituents carrying respectively a donor dimethylamino and an acceptor cyanoacrilic group as in **49** (Figure 16) [24] shows a shift towards less negative energy of the HOMO levels while the energy of the LUMO level is quite unaffected when compared to the corresponding mono β substituted $Zn^{II}$ porphyrin **14** (Figure 6), thus producing a decrease of the HOMO-LUMO energy gap [24]. However the HOMO-LUMO energy gap of a push pull 2,12 β disubstituted $Zn^{II}$ porphyrinic architecture is higher than that of the corresponding push pull 5,15

*meso* disubstituted $Zn^{II}$ porphyrinic architecture carrying the same donor and acceptor substituents [24], confirming that this push-pull electronic effect can be more easily transmitted through the 5,15 *meso* than the 2,12 pyrrolic positions of the porphyrinic ring, as also highlighted by the second order NLO behaviour of these two different kind of porphyrins [60].

Such limited electronic effect, is not unexpected since already Kim et al. [98] have reported that the introduction of an electron donor group into the β substituent has almost no influence on the HOMOs and LUMOs levels of β monosubstituted $Zn^{II}$ tetraarylporphyrins.

The shift to less negative energy of the HOMO and HOMO-1 levels and in particular of the HOMO-2 (usually at too low energy to be considered) is to be ascribed to the significant electron density on the substituent carrying the dimethylamino group. The HOMO-2 level of **49**, which has not a spatial analogue in the Gouterman model, is characterized also by a significant electron density on the porphyrinic core, differently from the HOMO-2 level of the structurally related $Zn^{II}$ tetraarylporphyrin **14** carrying only the acceptor ethynyl phenyl β substituent [24].

Very recently it was shown that a fine tuning of the HOMO and LUMO levels and of the push-pull character of a β substituted $Zn^{II}$ porphyrinic structure can be obtained also by acting on the electronic nature of the four aryl substituents in the *meso* positions of the porphyrinic ring. For instance for a new kind of push-pull 4D-π-1A type green β substituted $Zn^{II}$ porphyrins (**2** and **3** in Scheme 5) it was shown that substitution at the *meso* positions of the traditional sterically hindered 3,5-di-*tert*-butylphenyl substituent with a donating aryl substituent such as bis(4-*tert*-butylphenyl) aniline, produces a significant electronic effect by destabilizing the energy of the HOMO levels with parallel decrease of HOMO-LUMO energy gap [33].

Moreover the substitution in the π linker of a phenyl moiety with an acceptor benzothiadiazolic moiety (BTD) as in **3** (see Scheme 5) induces a stabilization of the LUMO levels with a further significant decrease of HOMO-LUMO gap (from 1.94 to 1.82 eV), which controls the position of the Q absorption band at lower energy, origin of the color of the porphyrinic dye.

It appears thus that by increasing the donor properties of the aryl substituents in the four *meso* positions and the acceptor properties of the π system of the β substituent, the push-pull character and the electronic absorption spectrum of this kind of $Zn^{II}$ porphyrins could be quite nicely tuned.

**5. Electron Transfer Kinetics**

The first attempt to gain structure/activity relationships involving charge transfer dynamics from a series of natural β-substituted chlorophyll derivatives, and their slightly modified synthetic derivatives (Figure 25) dates back to 1993 [64]. Chlorophylla (**67**) does not adsorb efficiently on $TiO_2$ from most of polar organic solvents, due to the weak interaction of the ester and keto carbonyl groups with the oxide surface. However adsorption takes place quite efficiently ($A_{670}$ = 0.3) from diethyl ether or hexane solutions. The absorption spectrum of **67** on $TiO_2$ is broadened and red shifted compared to the absorption spectrum in solution, probably due to the interaction with the surface and to dye aggregation. The IPCE spectrum at 670 nm is low (about 3.5%) in the presence of pyridine which, acting as an axial Mg ligand, reduces dye aggregation and excited state quenching.

Pheophytin (**68**), the free base of chlorophyll, shows a similarly poor photosensitization behaviour. The carboxylic group of pheophorbide (**69**) allows a much stronger adsorption onto $TiO_2$, resulting in an optical density of the photoanode at 675 nm (corresponding to the lowest singlet excited state Q band), of the order of 0.7. Despite this, the IPCE at 675 nm of only 25 %, was far behind the unit quantum efficiency for natural photosynthesis. Under the hypothesis that the propionic acid side chain might act as an insulating barrier for charge injection into the conduction band of $TiO_2$, chlorophyll derivatives with a carboxylic acid directly linked to the β pyrrolic position of the π electron system of the tetrapyrrole macrocycle, were investigated (**70**-**72**). The free base chlorin $e_6$ (**71**) and Cu chlorin (**72**) resulted in good efficiencies in the whole visible region, with an IPCE value up to 70 % for **72** at 650 nm. However, the presence of carboxylic anchoring group directly

linked at the β pyrrolic position could not be considered entirely responsible for the good quantum efficiencies, since, for example, Cu-2-α-oxymesochlorin (**73**), obtained as a major product from saponification of raw chlorophyll in the presence of $Cu^{2+}$, gave very similar IPCE values (up to 70 % at 630 nm). Based on these evidences, a direct link of the anchoring carboxylic group to the porphyrin ring did not seem strictly necessary for efficient electron injection into the photoanode. Detailed investigations based on sub-nanosecond laser spectroscopy [99] have demonstrated that non fluorescent chlorophyll derivatives like Cu chlorins (as **72**) have smaller charge injection rate constants ($k_{inj}$ = 3 $10^8$ $s^{-1}$) than porphyrinic systems injecting from singlet states like the free base chlorin $e_6$ (**67**) ($k_{inj}$ = 2.2 $10^9$ $s^{-1}$), although the longer lived triplet state of Cu chlorins still allows an high electron injection quantum yield. Moreover competitive excited state quenching due to exciton migration and annihilation was reduced with metal porphyrins undergoing efficient intersystem crossing, since long range energy transfer (Förster type) is spin forbidden. In the case of **73**, interesting photon to current conversion yields were reached in the red part of the adsorption spectrum, with overall efficiencies of 2.6 % ($J_{sc}$ = 9.4 mA/$cm^2$, $V_{oc}$ = 530 mV ) under full sunlight (0.1 W/$cm^2$).

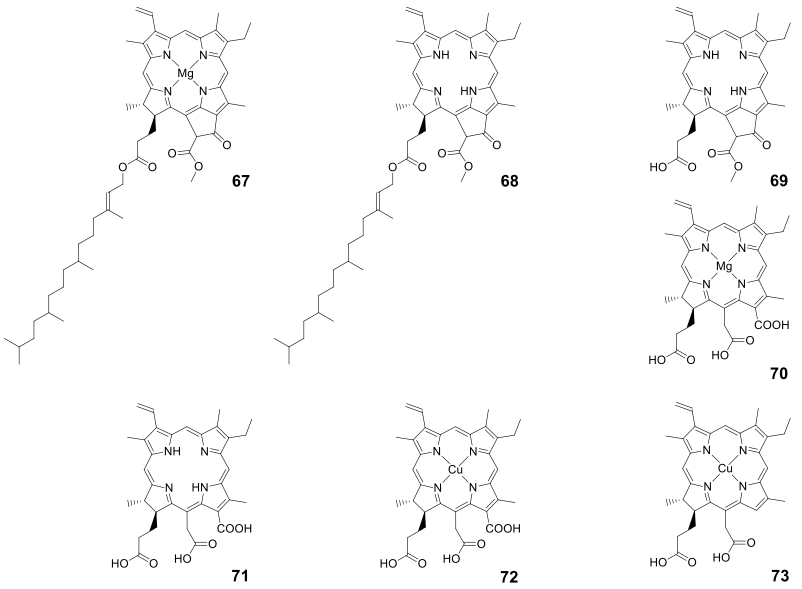

**Figure 25.** Structure of a series of natural chlorophyll derivatives bearing at least one linker group in β position: (**67**) chlorophyll a; (**68**) pheophytin; (**69**) Pheophorbide a; (**70**) Mg chlorin $e_6$ (**71**) chlorin $e_6$; (**72**) Cu chlorine $e_6$; (**73**) Cu-2-α-oxymesochlorin.

Mozer, Mori *et al.* [36] comparatively investigated the dynamics of series of synthetic β and *meso* substituted $Zn^{II}$ porphyrins. The best results were found in the case of **75** (Figure 26), delivering an efficiency of 6.1 % and maximum IPCE close to 70 % (Soret Band excitation) in optimized conditions, which is however lower than that obtained with the reference N719 ruthenium dye.

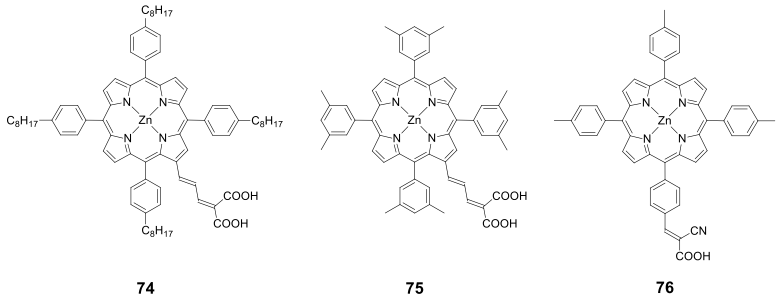

**Figure 26.** Examples of structures of porphyrin sensitizers considered by Mozer, Mori *et. al.* for ultrafast $TiO_2$ sensitization studies compared with N719 [36].

Ultrafast injection studies monitoring the NIR absorption of injected electrons, to avoid any interference from excited state signatures, showed that at least a fraction of porphyrin **75** was able to inject within the time resolution of the spectrometer (200 fs), but that the amplitude of the signal was lower than that obtained with N719 (when consideration was made for the amount of absorbed photons), consistent with maximum IPCE value < 100 % in the region where light harvesting was essentially unitary. A second rise due to a slower injection process in the ps region was also observed. Although the appearance of a slower component has been often observed in the case of N719 [100], and ascribed to injection from the excited triplet state, populated on ultrafast time scales, in the case of porphyrins the involvement of the lowest triplet as injecting state is generally ruled out for both free base and $Zn^{II}$ porphyrins [101]. Rather, it is plausible that multiple injection rates are in kinetic competition with excited state deactivation depending on the distribution of adsorption sites of the porphyrin dye on the $TiO_2$ surface and, in general, on surface heterogeneity of the mesoporous film. Nevertheless, at the microscopic level, the details of the influence of surface interactions on the injection yield remain quite elusive. It was also found a dependence of the charge injection kinetics on electrolyte composition, generally resulting in better injection quantum yields in the presence of higher $Li^+$ concentration (for example when moving from 0.1 to 0.7 M $Li^+$ the injection quantum yield of **75** improved by 20 %, Figure 27). This evidence indicates a better electron injection probably due to positive conduction band edge shift, so that a fine tuning of the electrolyte composition is necessary to extract optimal performance by a given molecular dye.

Codice campo modificato

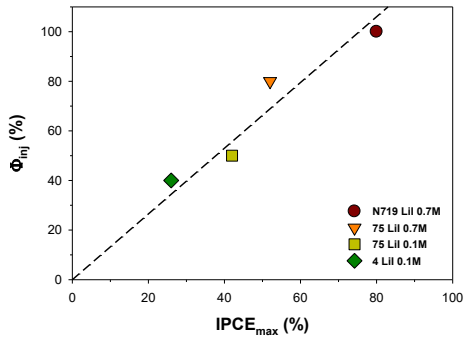


**Figure 27.** Electron injection yield determined form ultrafast kinetics versus maximum IPCE for **75** in comparison with dyes N719 and **4** reported in Figure 4 [102].

Charge recombination pathways could also represent limiting factors in porphyrins sensitized DSSCs, mainly as a result of electron recapture from acceptor states in the electrolyte (namely $I_3^-$ in case of iodide based electrolytes). In the case of porphyrinic dyes, favorable interactions between $I_3^-$ and the $Zn^{II}$ central ion of the porphyrin, and dispersive interactions between the polarizable conjugated π linker and $I_3^-$ may result in increased local concentration of $I_3^-$ in the vicinity of $TiO_2$ surface, where electron recombination could more easily occur. Indeed electron lifetimes by porphyrin sensitizers are often shorter than those found with ruthenium sensitized solar cells [36].

To address the relevance of the electron recapture process to the porphyrin sensitized solar cells, the electron transfer dynamics of a 2-β-substituted tetraarylporphyrinic dye (**14**) and a 5,15-*meso*-push-pull disubstituted diarylporphyrinic one (**17**) (reported in Figure 7) at the electrolyte/Dye/$TiO_2$ surface, were investigated [68].

Interestingly, significantly superior power conversion efficiencies where obtained for **14** (6.1%) with respect to **17** (3.9%), by using the $I^-/I_3^-$ based electrolyte. Nevertheless charge injection yields into $TiO_2$, evaluated through static emission quenching techniques, were quite similar and ≥ 80 % for both dyes. The investigation of the regeneration efficiency by $I^-$, performed in the absence of both $I_3^-$ and applied potential, also afforded comparable results, in the range of 75-85%, showing

that iodide can reduce both the oxidized dyes on the same timescale. These data were thus consistent with experimental IPCE data, corresponding to maximum monochromatic conversion efficiency ranging between 60 and 70%.

Conversely, major differences emerged by evaluating the electron lifetime, pointing out a slower charge recombination rate when **14** is adsorbed on $TiO_2$ (Figure 28). The electron lifetime ($\tau$) is expressed according to $\tau = R_{CT} \times C_{\mu}$, where $R_{CT}$ is the recombination resistance of $TiO_2$ and $C_{\mu}$ is its chemical capacitance [103], which is related to the density of electronically occupied states of the semiconductor. It follows that long electron lifetimes are achieved when both $R_{CT}$ and $C_{\mu}$ are maximized, *i.e.* recombination is slow while the population of injected electron into $TiO_2$ is increased, so that $\tau$ is a measurement of the quality of the dye sensitized interface with respect to recombination involving both the oxidized dye and the electrolyte. The observation of longer electron lifetime in DSSCs based on the dye **14** could be ascribed to an intrinsic superior passivation of the $TiO_2$ surface against charge recombination involving electron accepting species of the electrolyte. A superior screening effect, as well as reduced $\pi$-staking aggregation, are originated, as shown by computational modelling (Figure 29), by the higher steric hindrance of the tetraaryl porphyrinic architecture of the β-substituted dye, arising from the presence of four bulky *tert*-butyl-substituted aryl rings surrounding the porphyrinic core. Conversely, the pseudo linear 5,15 *meso* disubstituted push-pull diarylporphyrinic dye **17** features a lower sterical crowding, while the presence of the push-amino group may promote the formation of acid-base adducts with the $I_3^-$ ion, favouring either oxidative quenching of the excited state of the dye or recombination processes with the electrons of the photoanode, due to an increased local surface excess of $I_3^-$. Hence, it was reasonable to conclude that the better performance of DSSCs based on **14** with respect to **17**, was depending mainly on a significant reduction of the recombination rate with the oxidized redox mediator rather than on differences in regeneration efficiency or charge injection yield of the dye.

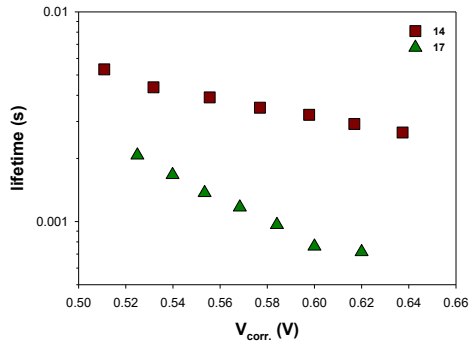


**Figure 28.** Electron lifetimes in **14** and **17** sensitized solar cells as a function of the corrected voltage ($V_{app}$-$iR_s$) where $R_s$ is the sum of serial resistance contributions.[68]

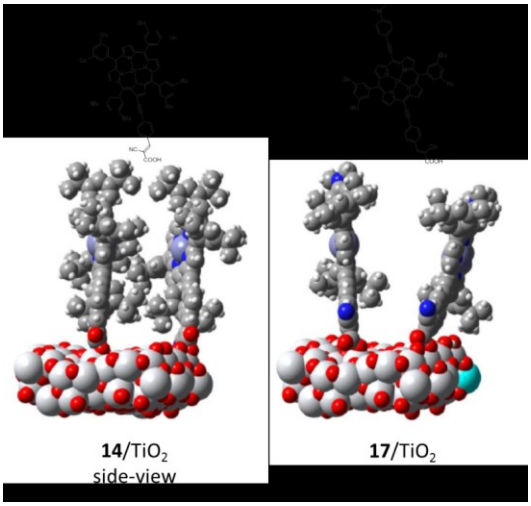


**Figure 29.** Space filling models of **14** and **17** (computed at the DFT-B3lyp-LANL2DZ levels) adsorbed on a $Ti_{36}O_{72}$ cluster [68].

The investigation of the charge transfer dynamics endowed with β and *meso* porphyrin structures was later extended to the structures of dyes **14 (**Figure 6**)**, **32 (**Figure 12**)** and **77** (Figure 30), where a highly conjugated bridge, characterized by the presence of a π-conjugated dithienylethylene

(DTE) unit, harvests a sizable portion of the visible spectrum around 500-550 nm, where more conventional β and *meso* porphyrins usually display a poor harvesting [104].

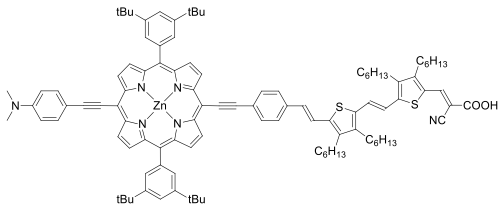


**77**

**Figure 30.** Molecular structure of porphyrinic dye **77**.

The excitation of these dyes in the absorption range between the B and Q band, where the spectral contribution of DTE is most significant, populates charge transfer (CT) states which undergo internal conversion to the lowest singlet state excited state (S1) with time constants $\tau_{ic}$ ranging from the sub-picosecond (major) to 10 ps (minor). The lowest singlet state decays according to a monoexponential kinetics with a lifetime of 1.6 ns. Population of the lowest triplet state (T1) proceeds at the sub-ns time scale, with intersystem crossing time constant $\tau_{isc}$ ranging from 130 ps (**14**) to ca. 400 ps (**77**, **32**). The triplet state survives for several hundred ns in aerated solution but is not involved in the process of electron injection. The excited state deactivation dynamics shares common features within the explored series which are schematized in Figure 31.

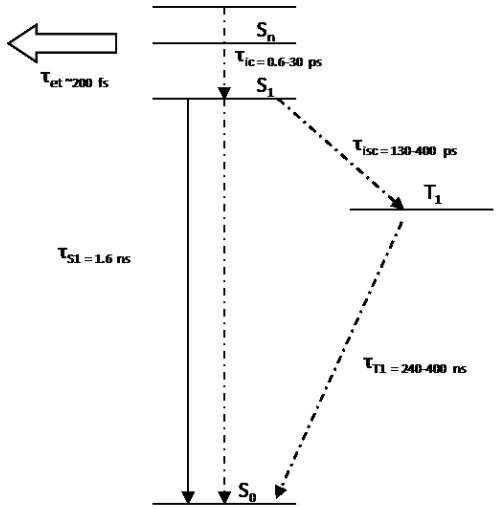


**Figure 31.** Schematic energy levels and deactivation time constants for the processes leading to deactivation of the excited states in the dyes **32** and **77,** carrying two DTE units in the β pendant, reported in Figures 12 and 30.

Excitation of the CT manifold bearing contributions by the DTE moiety results in electron injection into the $TiO_2$ surface on a time scale of ca. 200 fs, suggesting nearly quantitative deactivation of the singlet states by fast electron transfer. Such electron transfer kinetics is very similar to that of **14** which bears a much shorter acceptor pendant. The charge separated state on $TiO_2$ partly recombines according to a fast electron recapture kinetics in the ps timescale, while another fraction of the oxidized dye population survives well beyond the microsecond time scale being still incomplete on a time scale of $2\times10^{-5}$ s.

Interestingly the observation of a ps-ns recapture kinetics is consistent with reports from other authors about the charge recombination dynamics in organic push pull sensitizers [105], including different types of conjugated porphyirins [106], but could be exacerbated by the extreme power density achieved in sub-ps pump probe experiments.

On the other hand, the long lived fraction of the photogenerated oxidized dye can be nearly quantitatively intercepted by iodide, leading to regeneration efficiencies approaching unity (97% for **32**, 90% for **77** and 92% for **14**, at short circuit). Consistent with such photophysical observations, under low intensity monochromatic excitation, typical of IPCE measurements, quantum yields approaching 80 % where observed with the dyes **32** and **77** within the 500-550 nm spectral region, where the absorption of more common porphyrin designs, lacking the DTE moieties, would display poor harvesting and conversion. This is a confirmation that under short circuit conditions $\eta_{collection} \times \Phi_{inj}$ approaches unity for both the **77** and **32** dyes. Nevertheless fast recombination between photoinjected electrons and the oxidized porphyrin may be a limitation to cell efficiency under intense illumination and far from short circuit conditions, where the electron population inside the $TiO_2$ photoanode becomes more significant [102, 107].

Finally, it must be pointed out that it was not observed any significant impact of the substitution position (either β or *meso*) on the elementary steps of electron transfer kinetics comprising charge injection, dye regeneration and charge recombination. A very long π conjugated arm may however result in the activation of a channel of fast charge recombination, due to through space back electron transfer involving adjacent nanoparticles in the mesoscopic film. In the case of the DTE based conjugated pendant, this potential drawback is more than compensated by extended spectral sensitization and efficient injection by panchromatic states.

It can be thus concluded that the structural modification of a porphyrinic dye by adding an additional chromophore in either β or *meso* position has met the goal of extending the spectral light harvesting of the dye without introducing a kinetic barrier to charge injection and/or to dye regeneration. Under this respect, it appears clearly that β substitution represents a viable strategy for achieving dyes characterized by excellent photophysical properties, even with respect to 5,15-*meso* push-pull disubstituted structures, at the price of a reasonable synthetic complexity.

## 6. Conclusions

The aim of this review is to survey the recent advances in the development of porphyrin-based dyes with particular interest in their application on building integrated photovoltaics. In this specific context a rational design of the dyes has to meet some requirements for a large scale production: i) effectiveness of the synthetic procedures allowing large scale production; ii) good light-harvesting properties to promote adequate light-to-power conversion efficiencies; iii) good looking color to favor a pleasant lighting of the smart windows; iv) long term stability.

Although porphyrin dyes having a push-pull system arranged on the *meso* substitution pattern have been reported to apparently show the best performances in lab-scale DSSCs when compared, in the same conditions, with tetraaryl β substituted porphyrins or other unconventional porphyrin structures, they exhibited comparable photon-to-current efficiencies. Besides their considerable performances, the tetraaryl β substituted porphyrinic dyes can be obtained by facile and effective synthesis thanks to their highly symmetric core making them the most promising building blocks for a large scale production. Moreover in several studies a rational tailoring of the tetraaryl porphyrinic core and a judicious design of the substituents in β-pyrrolic position have been demonstrated to strongly impact the light harvesting properties, the electrochemical, the photophysical and the photoelectrochemical characteristics of the dyes.

In this review the recent findings about β-substituted porphyrin dyes have been surveyed to highlight the most significant features which have an effect on reducing the fabrication costs and on increasing the DSSC performances. The synthetic pathways of the most relevant dyes have been compared in order to screen the less demanding procedures which could be likely more profitable for industrial application. The influence on the HOMO-LUMO energy gaps, on the spectroscopic properties and on DSSC performances of various porphyrin cores, β-substituents and their relative connecting π-bridges as well as diverse types of anchoring groups have been extensively discussed.

Finally, the photophysical investigations on electron transfer kinetics at the semiconductor/dye/electrolytes interface have been also explored with particular attention to the role of the porphyrinic structure on electron transfer processes.

After a rapid screening of a wide range of porphyrinic dyes we have shown that tetraaryl β-ethynyl substituted ones could be considered as promising DSSC photosensitizers for industrial application on BIPV. In fact, concerning the fabrication costs, they can take advantages from the highly symmetric tetraarylporphyrin core and the facile linking of ethynyl π-extended systems on β-pyrrolic position allowing cost-effective synthetic pathways. In this kind of dyes the sterically hindered macrocyclic core is also able to guarantee an excellent passivation of the photoanode reducing the charge recombination at the $TiO_2$ surface due to the approaching of oxidized species from electrolyte. Moreover the comparison of the photophysical properties of β- and *meso*-substituted porphyrins has not revealed any significant differences in the rate of other charge transfer processes as electron injection yields and regeneration efficiencies. Finally the electronic properties of the dyes can be easily tuned by acting both on the chemical structure of tetraarylporphyrin core and on the nature of substituents in pyrrolic positions thus influencing their HOMO-LUMO energy gaps. These are strictly related to the push-pull character of the dyes and to their spectroscopic properties which impact both on their colour and on their light-harvesting capacity.

With this review we don't want to establish which kind of porphyrinic structures is best performing in DSSCs but which of them meet the requirements to move the production from the lab- to the industrial-scale for the fabrication of PV windows. We strongly believe that the teraaryl β substituted porphyrins present the more suitable characteristics for this purpose and we want to encourage the scientific community for future advances in this area opening the way for further investigation and optimization of this promising class of sensitizers.

**Acknowledgement**

This research did not receive any specific grant from funding agencies in the public, commercial, or not-for-profit sectors. We thank Prof. Renato Ugo for useful discussions over the preparation of this review.

**References**

[1] J. Benemann, O. Chehab, E. Schaar-Gabriel, Sol. Energy Mater. Sol. Cells, 67 (2001) 345-354.

[2] A. Hinsch, H. Brandt, W. Veurman, S. Hemming, M. Nittel, U. Würfel, P. Putyra, C. Lang-Koetz, M. Stabe, S. Beucker, K. Fichter, Sol. Energy Mater. Sol. Cells, 93 (2009) 820-824.

[3] B. O'Regan, M. Grätzel, Nature, 353 (1991) 737-740.

[4] A. Hagfeldt, G. Boschloo, L. Sun, L. Kloo, H. Pettersson, Chem. Rev., 110 (2010) 6595-6663.

[5] W.M. Campbell, A.K. Burrell, D.L. Officer, K.W. Jolley, Coord. Chem. Rev., 248 (2004) 1363-1379.

[6] K. Hara, Molecular Design of Sensitizers for Dye-Sensitized Solar Cells, in: T. Okada, M. Kaneko (Eds.) Molecular Catalysts for Energy Conversion, Springer-Verlag Berlin, Berlin, 2009, pp. 217-250.

[7] V. Balzani, A. Credi, M. Venturi, Chemsuschem, 1 (2008) 26-58.

[8] S. Caramori, C.A. Bignozzi, Recent Developments in the Design of Dye-Sensitized Solar Cell Components, in: Electrochemistry of Functional Supramolecular Systems, John Wiley & Sons, Inc., 2010, pp. 523-579.

[9] C.A. Bignozzi, R. Argazzi, R. Boaretto, E. Busatto, S. Carli, F. Ronconi, S. Caramori, Coord. Chem. Rev., 257 (2013) 1472-1492.

[10] M. Victoria Martinez-Diaz, G. de la Torrea, T. Torres, Chem. Commun., 46 (2010) 7090-7108.

[11] M. Freitag, J. Teuscher, Y. Saygili, X. Zhang, F. Giordano, P. Liska, J. Hua, S.M. Zakeeruddin, J.-E. Moser, M. Grätzel, A. Hagfeldt, Nature Photonics, 11 (2017) 372.

[12] F. Viola, P. Romano, R. Miceli, E.R. Sanseverino, G. Perrone, R. Corrao, M. Morini, L. Pastore, J. Pidanic, in: 2015 Tenth International Conference on Ecological Vehicles and Renewable Energies (EVER), 2015, pp. 1-5.

[13] A.J. Marszal, P. Heiselberg, J.S. Bourrelle, E. Musall, K. Voss, I. Sartori, A. Napolitano, Energy and Buildings, 43 (2011) 971-979.

[14] I. Sartori, A. Napolitano, K. Voss, Energy and Buildings, 48 (2012) 220-232.

[15] D.H.W. Li, L. Yang, J.C. Lam, Energy, 54 (2013) 1-10.

[16] A. Colombo, G. Di Carlo, C. Dragonetti, M. Magni, A. Orbelli Biroli, M. Pizzotti, D. Roberto, F. Tessore, E. Benazzi, C.A. Bignozzi, L. Casarin, S. Caramori, Inorg. Chem., (2017).

[17] M.K. Nazeeruddin, A. Kay, I. Rodicio, R. Humphry-Baker, E. Müller, P. Liska, N. Vlachopoulos, M. Grätzel, J. Am. Chem. Soc., 115 (1993) 6382.

[18] M.K. Nazeeruddin, F. De Angelis, S. Fantacci, A. Selloni, G. Viscardi, P. Liska, S. Ito, B. Takeru, M. Grätzel, J. Am. Chem. Soc., 127 (2005) 16835-16847.

[19] Q. Yu, Y. Wang, Z. Yi, N. Zu, J. Zhang, M. Zhang, P. Wang, Acs Nano, 4 (2010) 6032-6038.

[20] K. Kakiage, Y. Aoyama, T. Yano, K. Oya, J.-i. Fujisawa, M. Hanaya, Chem. Commun., 51 (2015) 15894-15897.

[21] A. Yella, H.-W. Lee, H.N. Tsao, C. Yi, A.K. Chandiran, M.K. Nazeeruddin, E.W.-G. Diau, C.-Y. Yeh, S.M. Zakeeruddin, M. Grätzel, Science, 334 (2011) 629-634.

[22] S. Mathew, A. Yella, P. Gao, R. Humphry-Baker, F.E. CurchodBasile, N. Ashari-Astani, I. Tavernelli, U. Rothlisberger, K. NazeeruddinMd, M. Grätzel, Nature Chemistry, 6 (2014) 242-247.

[23] A. Yella, C.-L. Mai, S.M. Zakeeruddin, S.-N. Chang, C.-H. Hsieh, C.-Y. Yeh, M. Grätzel, Angew. Chem. Int. Ed., 53 (2014) 2973-2977.

[24] G. Di Carlo, A. Orbelli Biroli, M. Pizzotti, F. Tessore, V. Trifiletti, R. Ruffo, A. Abbotto, A. Amat, F. De Angelis, P.R. Mussini, Chem. Eur. J., 19 (2013) 10723-10740.

[25] A. Orbelli Biroli, F. Tessore, M. Pizzotti, C. Biaggi, R. Ugo, S. Caramori, A. Aliprandi, C.A. Bignozzi, F. De Angelis, G. Giorgi, E. Licandro, E. Longhi, J. Phys. Chem. C, 115 (2011) 23170-23182.

[26] C.-F. Lo, S.-J. Hsu, C.-L. Wang, Y.-H. Cheng, H.-P. Lu, E.W.-G. Diau, C.-Y. Lin, J. Phys. Chem. C, 114 (2010) 12018-12023.

[27] T. Bessho, S.M. Zakeeruddin, C.-Y. Yeh, E.W.-G. Diau, M. Grätzel, Angew. Chem. Int. Ed., 49 (2010) 6646-6649.

[28] Y.-C. Chang, C.-L. Wang, T.-Y. Pan, S.-H. Hong, C.-M. Lan, H.-H. Kuo, C.-F. Lo, H.-Y. Hsu, C.-Y. Lin, E.W.-G. Diau, Chem. Commun., 47 (2011) 8910-8912.

[29] C.-L. Wang, C.-M. Lan, S.-H. Hong, Y.-F. Wang, T.-Y. Pan, C.-W. Chang, H.-H. Kuo, M.-Y. Kuo, E.W.-G. Diau, C.-Y. Lin, Energy Environ. Sci., 5 (2012) 6933-6940.

[30] W.M. Campbell, K.W. Jolley, P. Wagner, K. Wagner, P.J. Walsh, K.C. Gordon, L. Schmidt-Mende, M.K. Nazeeruddin, Q. Wang, M. Grätzel, D.L. Officer, J. Phys. Chem. C, 111 (2007) 11760-11762.

[31] G. Di Carlo, A. Orbelli Biroli, F. Tessore, M. Pizzotti, P.R. Mussini, A. Amat, F. De Angelis, A. Abbotto, V. Trifiletti, R. Ruffo, J. Phys. Chem. C, 118 (2014) 7307-7320.

[32] A. Orbelli Biroli, F. Tessore, V. Vece, G. Di Carlo, P.R. Mussini, V. Trifiletti, L. De Marco, R. Giannuzzi, M. Manca, M. Pizzotti, J. Mater. Chem. A, 3 (2015) 2954-2959.

[33] A. Covezzi, A. Orbelli Biroli, F. Tessore, A. Forni, D. Marinotto, P. Biagini, G. Di Carlo, M. Pizzotti, Chem. Commun., 52 (2016) 12642-12645.

[34] L.L. Li, E.W.G. Diau, Chem. Soc. Rev., 42 (2013) 291-304.

[35] T. Higashino, H. Imahori, Dalton Trans., 44 (2015) 448-463.

[36] M.J. Griffith, K. Sunahara, P. Wagner, K. Wagner, G.G. Wallace, D.L. Officer, A. Furube, R. Katoh, S. Mori, A.J. Mozer, Chem. Commun., 48 (2012) 4145-4162.

[37] K. Ladomenou, T.N. Kitsopoulos, G.D. Sharma, A.G. Coutsolelos, RSC Advances, 4 (2014) 21379-21404.

[38] K. Kurotobi, Y. Toude, K. Kawamoto, Y. Fujimori, S. Ito, P. Chabera, V. Sundström, H. Imahori, Chem. - Eur. J., 19 (2013) 17075-17081.

[39] Q. Arooj, G.J. Wilson, F. Wang, RSC Adv., 6 (2016) 15345-15353.

[40] C.-Y. Huang, C.-Y. Hsu, L.-Y. Yang, C.-J. Lee, T.-F. Yang, C.-C. Hsu, C.-H. Ke, Y.O. Su, European Journal of Inorganic Chemistry, 2012 (2012) 1038-1047.

[41] R.B. Ambre, S.B. Mane, G.-F. Chang, C.-H. Hung, ACS Appl. Mater. Interfaces, 7 (2015) 1879-1891.

[42] M.O. Senge, Chem. Commun., 47 (2011) 1943-1960.

[43] J.S. Lindsey, Acc. Chem. Res., 43 (2010) 300-311.

[44] L.-H. Han, C.-R. Zhang, J.-W. Zhe, N.-Z. Jin, Y.-L. Shen, W. Wang, J.-J. Gong, Y.-H. Chen, Z.-J. Liu, International Journal of Molecular Sciences, 14 (2013) 20171.

[45] Y.Y. Enakieva, J. Michalak, I.A. Abdulaeva, M.V. Volostnykh, C. Stern, R. Guilard, A.G. Bessmertnykh-Lemeune, Y.G. Gorbunova, A.Y. Tsivadze, K.M. Kadish, European Journal of Organic Chemistry, 2016 (2016) 4881-4892.

[46] G. Di Carlo, A. Orbelli Biroli, F. Tessore, S. Rizzato, A. Forni, G. Magnano, M. Pizzotti, The Journal of Organic Chemistry, 80 (2015) 4973-4980.

[47] H.J. Callot, Tetrahedron Lett., 14 (1973) 4987-4990.

[48] Q. Wang, W.M. Campbell, E.E. Bonfantani, K.W. Jolley, D.L. Officer, P.J. Walsh, K. Gordon, R. Humphry-Baker, M.K. Nazeeruddin, M. Grätzel, The Journal of Physical Chemistry B, 109 (2005) 15397-15409.

[49] J.S. Lindsey, I.C. Schreiman, H.C. Hsu, P.C. Kearney, A.M. Marguerettaz, The Journal of Organic Chemistry, 52 (1987) 827-836.

[50] M. Ishida, D. Hwang, Z. Zhang, Y.J. Choi, J. Oh, V.M. Lynch, D.Y. Kim, J.L. Sessler, D. Kim, Chemsuschem, 8 (2015) 2967-2977.

[51] M. Ishida, D. Hwang, Y.B. Koo, J. Sung, D.Y. Kim, J.L. Sessler, D. Kim, Chemical Communications, 49 (2013) 9164-9166.

[52] A.W.I. Stephenson, P. Wagner, A.C. Partridge, K.W. Jolley, V.V. Filichev, D.L. Officer, Tetrahedron Lett., 49 (2008) 5632-5635.

[53] H. Hayashi, A.S. Touchy, Y. Kinjo, K. Kurotobi, Y. Toude, S. Ito, H. Saarenpää, N.V. Tkachenko, H. Lemmetyinen, H. Imahori, Chemsuschem, 6 (2013) 508-517.

[54] R.G.W. Jinadasa, Y. Fang, S. Kumar, A.J. Osinski, X. Jiang, C.J. Ziegler, K.M. Kadish, H. Wang, The Journal of Organic Chemistry, 80 (2015) 12076-12087.

[55] R.G. Waruna Jinadasa, M.B. Thomas, Y. Hu, F. D'Souza, H. Wang, Physical Chemistry Chemical Physics, (2017).

[56] G. Magnano, D. Marinotto, M.P. Cipolla, V. Trifiletti, A. Listorti, P.R. Mussini, G. Di Carlo, F. Tessore, M. Manca, A. Orbelli Biroli, M. Pizzotti, PCCP, 18 (2016) 9577-9585.

[57] G.Y. Gao, Y. Chen, X.P. Zhang, The Journal of Organic Chemistry, 68 (2003) 6215-6221.

[58] E. Annoni, M. Pizzotti, R. Ugo, S. Quici, T. Morotti, M. Bruschi, P. Mussini, Eur. J. Inorg. Chem., 2005 (2005) 3857-3874.

[59] H. Shahroosvand, S. Zakavi, A. Sousaraei, M. Eskandari, PCCP, 17 (2015) 6347-6358.

[60] A. Orbelli Biroli, F. Tessore, S. Righetto, A. Forni, A. Macchioni, L. Rocchigiani, M. Pizzotti, G. Di Carlo, Inorg. Chem., 56 (2017) 6438-6450.

[61] A. Sen, V. Krishnan, Tetrahedron Lett., 37 (1996) 8437-8438.

[62] I.D.L. Albert, T.J. Marks, M.A. Ratner, Chem. Mater., 10 (1998) 753-762.

[63] L. Karki, F.W. Vance, J.T. Hupp, S.M. LeCours, M.J. Therien, J. Am. Chem. Soc., 120 (1998) 2606-2611.

[64] A. Kay, M. Grätzel, Journal of Physical Chemistry, 97 (1993) 6272.

[65] M.K. Nazeeruddin, R. Humphry-Baker, D.L. Officer, W.M. Campbell, A.K. Burrell, M. Grätzel, Langmuir, 20 (2004) 6514-6517.

[66] Q. Wang, W.M. Campbell, E.E. Bonfantani, K.W. Jolley, D.L. Officer, P.J. Walsh, K. Gordon, R. Humphry-Baker, M.K. Nazeeruddin, M. Grätzel, J. Phys. Chem. B, 109 (2005) 15397-15409.

[67] T. Sakurada, Y. Arai, H. Segawa, RSC Advances, 4 (2014) 13201-13204.

[68] G. Di Carlo, S. Caramori, V. Trifiletti, R. Giannuzzi, L. De Marco, M. Pizzotti, A. Orbelli Biroli, F. Tessore, R. Argazzi, C.A. Bignozzi, ACS Applied Materials & Interfaces, 6 (2014) 15841-15852.

[69] V.K. Narra, H. Ullah, V.K. Singh, L. Giribabu, S. Senthilarasu, S.Z. Karazhanov, A.A. Tahir, T.K. Mallick, H.M. Upadhyaya, Polyhedron, 100 (2015) 313-320.

[70] C.A. Hunter, J.K.M. Sanders, J. Am. Chem. Soc., 112 (1990) 5525-5534.

[71] J.N. Clifford, E. Martinez-Ferrero, A. Viterisi, E. Palomares, Chem. Soc. Rev., 40 (2011) 1635-1646.

[72] M. Urbani, M. Grätzel, M.K. Nazeeruddin, T. Torres, Chem. Rev., 114 (2014) 12330-12396.

[73] A.J. Mozer, P. Wagner, D.L. Officer, G.G. Wallace, W.M. Campbell, M. Miyashita, K. Sunahara, S. Mori, Chem. Commun., (2008) 4741-4743.

[74] P.R. Mussini, A. Orbelli Biroli, F. Tessore, M. Pizzotti, C. Biaggi, G. Di Carlo, M.G. Lobello, F. De Angelis, Electrochim. Acta, 85 (2012) 509-523.

[75] V.A. Nuay, D.-H. Kim, S.-H. Lee, J.-J. Ko, Bull. Korean Chem. Soc., 30 (2009) 2871-2872.

[76] E.M. Barea, R. Caballero, L. López-Arroyo, A. Guerrero, P. de la Cruz, F. Langa, J. Bisquert, Chemphyschem, 12 (2011) 961-965.

[77] K. Sirithip, S. Morada, S. Namuangruk, T. Keawin, S. Jungsuttiwong, T. Sudyoadsuk, V. Promarak, Tetrahedron Lett., 54 (2013) 2435-2439.

[78] F. Lu, Y. Feng, X. Wang, Y. Zhao, G. Yang, J. Zhang, B. Zhang, Z. Zhao, Dyes and Pigments, 139 (2017) 255-263.

[79] H. Baba, J. Chen, H. Shinokubo, A. Osuka, Chemistry – A European Journal, 14 (2008) 4256-4262.

[80] M. Ishida, S.W. Park, D. Hwang, Y.B. Koo, J.L. Sessler, D.Y. Kim, D. Kim, J. Phys. Chem. C, 115 (2011) 19343-19354.

[81] M. Tanaka, S. Hayashi, S. Eu, T. Umeyama, Y. Matano, H. Imahori, Chem. Commun., (2007) 2069-2071.

[82] S. Hayashi, M. Tanaka, H. Hayashi, S. Eu, T. Umeyama, Y. Matano, Y. Araki, H. Imahori, J. Phys. Chem. C, 112 (2008) 15576-15585.

[83] S. Eu, S. Hayashi, T. Urneyama, Y. Matano, Y. Araki, H. Imahori, Journal of Physical Chemistry C, 112 (2008) 4396-4405.

[84] H. Imahori, T. Umeyama, S. Ito, Accounts of Chemical Research, 42 (2009) 1809-1818.

[85] A. Kira, Y. Matsubara, H. Iijima, T. Umeyama, Y. Matano, S. Ito, M. Niemi, N.V. Tkachenko, H. Lemmetyinen, H. Imahori, The Journal of Physical Chemistry C, 114 (2010) 11293-11304.

[86] H. Imahori, H. Iijima, H. Hayashi, Y. Toude, T. Umeyama, Y. Matano, S. Ito, Chemsuschem, 4 (2011) 797-805.

[87] C. Jiao, N. Zu, K.-W. Huang, P. Wang, J. Wu, Org. Lett., 13 (2011) 3652-3655.

[88] J.M. Ball, N.K.S. Davis, J.D. Wilkinson, J. Kirkpatrick, J. Teuscher, R. Gunning, H.L. Anderson, H.J. Snaith, RSC Advances, 2 (2012) 6846-6853.

[89] C.-L. Mai, W.-K. Huang, H.-P. Lu, C.-W. Lee, C.-L. Chiu, Y.-R. Liang, E.W.-G. Diau, C.-Y. Yeh, Chem. Commun., 46 (2010) 809-811.

[90] J.K. Park, J. Chen, H.R. Lee, S.W. Park, H. Shinokubo, A. Osuka, D. Kim, J. Phys. Chem. C, 113 (2009) 21956-21963.

[91] P.J. Walsh, K.C. Gordon, D.L. Officer, W.M. Campbell, Journal of Molecular Structure: THEOCHEM, 759 (2006) 17-24.

[92] J.C. Earles, K.C. Gordon, A.W.I. Stephenson, A.C. Partridge, D.L. Officer, PCCP, 13 (2011) 1597-1605.

[93] S.J. Lind, K.C. Gordon, S. Gambhir, D.L. Officer, PCCP, 11 (2009) 5598-5607.

[94] M.P. Balanay, D.H. Kim, Journal of Molecular Structure: THEOCHEM, 910 (2009) 20-26.

[95] M. Gouterman, The Journal of Chemical Physics, 30 (1959) 1139-1161.

[96] M. Gouterman, G.H. Wagnière, L.C. Snyder, J. Mol. Spectrosc., 11 (1963) 108-127.

[97] R. Ma, P. Guo, L. Yang, L. Guo, Q. Zeng, G. Liu, X. Zhang, Journal of Molecular Structure: THEOCHEM, 942 (2010) 131-136.

[98] M.P. Balanay, C.V.P. Dipaling, S.H. Lee, D.H. Kim, K.H. Lee, Sol. Energy Mater. Sol. Cells, 91 (2007) 1775-1781.

[99] A. Kay, R. Humphry-Baker, M. Graetzel, The Journal of Physical Chemistry, 98 (1994) 952-959.

[100] S.E. Koops, B.C. O'Regan, P.R.F. Barnes, J.R. Durrant, J. Am. Chem. Soc., 131 (2009) 4808-4818.

[101] Y. Tachibana, S.A. Haque, I.P. Mercer, J.R. Durrant, D.R. Klug, The Journal of Physical Chemistry B, 104 (2000) 1198-1205.

[102] K. Sunahara, A. Furube, R. Katoh, S. Mori, M.J. Griffith, G.G. Wallace, P. Wagner, D.L. Officer, A.J. Mozer, The Journal of Physical Chemistry C, 115 (2011) 22084-22088.

[103] J. Bisquert, PCCP, 5 (2003) 5360-5364.

[104] G. Di Carlo, S. Caramori, L. Casarin, A. Orbelli Biroli, F. Tessore, R. Argazzi, A. Oriana, G. Cerullo, C.A. Bignozzi, M. Pizzotti, J. Phys. Chem. C, 121 (2017) 18385-18400.

[105] J. Wiberg, T. Marinado, D.P. Hagberg, L. Sun, A. Hagfeldt, B. Albinsson, J. Phys. Chem. C, 113 (2009) 3881-3886.

[106] C.-W. Chang, L. Luo, C.-K. Chou, C.-F. Lo, C.-Y. Lin, C.-S. Hung, Y.-P. Lee, E.W.-G. Diau, J. Phys. Chem. C, 113 (2009) 11524-11531.

[107] K.C.D. Robson, K. Hu, G.J. Meyer, C.P. Berlinguette, J. Am. Chem. Soc., 135 (2013) 1961-1971.